PHOTOGRAPH THIS SHEET

AD-A951 689

DTIC ACCESSION NUMBER

LEVEL

1

INVENTORY

WAL
WAL 372/32
ARF 2182-12

DOCUMENT IDENTIFICATION

This document has been approved for public release and sale; its distribution is unlimited.

(1)

DISTRIBUTION STATEMENT

ACCESSION FOR	
NTIS	GRA&I
DTIC	TAB
UNANNOUNCED	
JUSTIFICATION	
(MAR 23 1961)	
BY	
DISTRIBUTION /	
AVAILABILITY CODES	
DIST	AVAIL AND/OR SPECIAL
A	

DISTRIBUTION STAMP

UNANNOUNCED

DTIC
ELECTE
S MAY 26 1982 D
E

DATE ACCESSIONED

DTIC COPY INSPECTED 2

82 05 25 053

DATE RECEIVED IN DTIC

PHOTOGRAPH THIS SHEET AND RETURN TO DTIC-DDA-2

DTIC FORM OCT 79 70A

DOCUMENT PROCESSING SHEET

ARF

ARMOUR RESEARCH FOUNDATION OF ILLINOIS INSTITUTE OF TECHNOLOGY

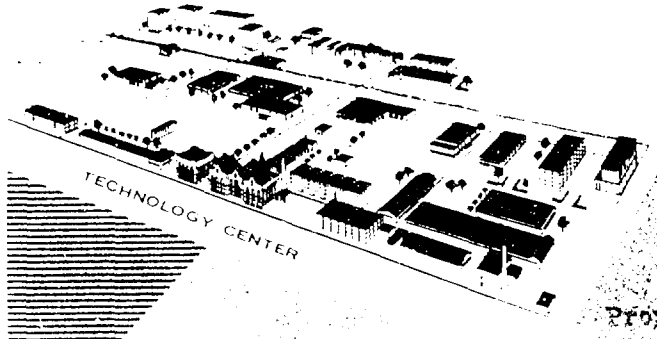

DEVELOPMENT AND APPLICATION OF A THEORY OF PLASTIC DEFORMATION OF CEMENTED ALLOYS

By
N. M. Parikh

March 23, 1961

Watertown Arsenal
Watertown 72, Massachusetts

Contract No. DA-11-022-505-ORD-3092
ORD Project No. TB4-002
D/A Project No. 5B93-32-002
TECHNICAL REPORT NO. WAL 372/32

Unclassified

ASTIA DOCUMENT NO. ~~256 608~~

FILING SUBJECTS:
alloys, refractory
alloys, cemented

TECHNICAL REPORT ARF 2182-12, WAL 372/32
COPY NUMBER _____

DEVELOPMENT AND APPLICATION OF A THEORY OF PLASTIC DEFORMATION OF CEMENTED ALLOYS

By

N. M. Parikh

March 23, 1961

Watertown Arsenal
Watertown 72, Massachusetts

Contract No. DA-11-022-505-ORD-3092
ORD Project No. TB4-002
D/A Project No. 5B93-32-002
TECHNICAL REPORT NO. WAL 372/32

Unclassified

Qualified requesters may obtain copies of report from the Armed Services Technical Information Agency, Arlington Hall Station, Arlington 12, Virginia.

DEVELOPMENT AND APPLICATION OF A THEORY OF PLASTIC DEFORMATION OF CEMENTED ALLOYS

ABSTRACT

An investigation was undertaken to study the fundamental reasons for room temperature ductility, and strength of the W-Ni-Fe alloys. Phase I of this program involved the development of the theory of plastic deformation of such alloys and Phase II will be concerned with the application of this theory to the development of new alloys.

In the cemented W-Ni-Fe alloys, the chemistry of the matrix alloy was established by the use of the electron probe analyser. The sources of strength and ductility of cemented structures in the W-Ni-Fe system were established by careful determination of yield strength - grain size relationship in the matrix alloy as well as tungsten and extrapolating the plots to the grain sizes of the components in the cemented structures. The work hardening characteristics of the components were also taken into account. The residual stresses in the cemented W-Ni-Fe alloys were calculated from precise measurements of the lattice parameters of matrix and tungsten as a function of gross composition. A cursory application of the principles derived to the development of new alloys based on tungsten and on iron showed the soundness of these principles and resulted in a few new Fe-Cu base alloys.

TABLE OF CONTENTS

LIST OF ILLUSTRATIONS

LIST OF ILLUSTRATIONS (Cont'd)

LIST OF TABLES

DEVELOPMENT AND APPLICATION OF A THEORY OF PLASTIC DEFORMATION OF CEMENTED ALLOYS

I. INTRODUCTION

The "cermet" type dispersed systems, wherein strong, hard particles are embedded in a more or less continuous phase of a ductile matrix, have been subjected to extensive investigations in the past decade. Systems in this category have found widespread applications in the carbide tool industry, in bearings, and in some structural parts. In spite of the high strengths of alloys such as WC-Co, TiC-Ni-Mo, W-Cu-Ni, etc., none of them have exhibited any degree of ductility at any temperature. One exception to this widespread rule was reported by Green et al.[1] They found that some compositions in the W-Ni-Fe system with about 90 weight per cent tungsten exhibited good room-temperature ductility and their strength characteristics were those of pure tungsten. For an extension of these attributes in the development of new systems, it must be understood quantitatively why the W-Ni-Fe system exhibits good room-temperature ductility and formability while its sister systems, such as W-Cu or W-Ni, do not.

Thus, the basic purpose of this investigation was to study the fundamental reasons for room-temperature ductility and strength of the W-Ni-Fe alloys and to attempt the application of these fundamentals to the development of new alloys. Phase I of this program involved the development of the theory of plastic deformation of such cemented alloys, and Phase II was to be concerned with the application of this theory to the development of new alloys.

In the current program, the objectives set forth in Phase I have been completed successfully. The chemistry of the alloys in the W-Ni-Fe system has

---

"Delivered by Armour Research Foundation of Illinois Institute of Technology pursuant to Contract No. DA-11-022-505-ORD-3092. Government's use controlled by the provisions of Articles 26 and 27 of Title II (General Provisions)."

been established by the electron probe microanalyzer. This helped in establishing the exact composition of the matrix alloy in the cemented structures. The sources of strength and ductility of compositions in the W-Ni-Fe system were established by careful determination of the yield strength vs. grain size relationships in the matrix alloy as well as tungsten and extrapolating the plots to the grain sizes of the components in the cemented structures. The work-hardening coefficients of the components were also measured. The residual stresses in the above-mentioned compositions were calculated from precise measurements of the lattice parameters of the components as a function of composition. A cursory application of the principles derived to the development of new alloys based on tungsten and on iron showed the soundness of these principles and resulted in a few new alloys. Thus the investigation has resulted in the establishment of a quantitative relationship between the primary sources of strength and ductility of such cemented structures.

II. THEORETICAL CONSIDERATIONS

Due to the rather large concentrations of the dispersed phase (greater than 65 volume per cent) and due to the large separation between the dispersed phase particles (greater than 1 micron) in cemented structures, the latter cannot be analyzed in terms of the theories of dispersion hardening. Therefore, a new approach for the analysis of such cemented structures was proposed in this program. As stated before, the cemented alloys (as, for example, in the W-Ni-Fe system) of high tungsten concentration are characterized by the discontinuous or semicontinuous dispersion of spherical tungsten grains in a continuous or semicontinuous matrix film (size of the order greater than 1 micron) of the Ni-Fe rich phase. Now, instead of considering the matrix as a "film" which is not subject to quantitative analysis - as has been the normal practice to date - if we consider the matrix to be a second phase whose effective grain size is the same as the average thickness of the matrix film in the cemented alloy, the problem becomes considerably more susceptible to analysis.

"Delivered by Armour Research Foundation of Illinois Institute of Technology pursuant to Contract No. DA-11-022-AMC-0HD-3092. Government's use controlled by the provisions of Articles 26 and 27 of Title II (General Provisions)."

First, let us examine the stress-strain response characteristics of two-phase alloys using Taylor's[2] postulates. In view of the fact that the alloys under investigation were two-phase, they may be compared with other two-phase systems which do not necessarily exhibit a cemented structure. The deformation of such alloys can take place by either of the two mechanisms: maintaining the stress continuity or maintaining the strain continuity. Although numerous investigations have been made on the plastic behavior of two-phase alloys, the data reported do not conclusively obey either of the two conditions exclusively.[3] It may well be that the deformation of polyphase alloys is partly isostrain and partly isostress because the two conditions of equilibrium of stresses and continuity of strains across the two-phase boundary must be satisfied simultaneously.

The work of Honeycomb and Boas[4] on α -β brass supports the isostress hypothesis for the deformation of a two-phase system. Clarebough,[5] on the other hand, in his work on Ag-Mg alloys and brass reports that the harder β phase was more extensively deformed near the boundary than in the center of the β crystal, and the deformation of the softer α phase was smaller in the vicinity of the β crystal. Moreover, the harder β phase deformed more at the same stress level in the presence of increasing amounts of softer α phase. This effect is partially in agreement with the continuity-of-strain hypothesis. A survey of the past literature indicates that the main difficulty in clear analysis of the deformation of two-phase alloys has been in the design of meaningful experiments to obtain unambiguous results with the use of the available experimental techniques.

There is considerable information in the literature on the effect of microstructure on the mechanical properties of two-phase alloys. Because the cemented alloys of the present investigation are somewhat like the Fe_3C dispersions in a continuous matrix of ferrite inasmuch as the matrix film thickness is considerably larger (greater than 1 micron) than called for in classically dispersion-hardened alloys (interparticle distance ~ 0.01 micron), the

---

"Delivered by Armour Research Foundation of Illinois Institute of Technology pursuant to Contract No. DA-11-022-505-ORD-3092. Government's use controlled by the provisions of Articles 26 and 27 of Title II (General Provisions)."

concepts developed for the dispersion-hardened alloys would no longer be tenable for the cemented alloys. A new approach has to be evolved for the analysis of such cemented alloys. The first systematic study of the effect of dispersions of carbides in ferrite was reported by Gensamer[6] and his colleagues. Essentially, their results show a reasonable correlation between the effective ferrite grain size (or Fe_3C-Fe_3C interparticle separation) and the yield strength of the composite alloy. Their data, within a broad scatter band, reveal that the yield strength of alloys with carbide dispersions in ferritic steels decreases linearly with the logarithm of the mean ferrite path, independent of carbon content or the shape of the dispersions. Their results are reproduced in Fig. 1. Thus the strength is purely a function of effective size of the ferrite grain. Of course, one must keep in mind that the effective size of these ferrite grains can be much smaller than the one which is observed metallographically if the interface between the carbide particles and ferrite matrix is in a state of high stress.

To date, there has been no quantitative investigation of the sources of strength and ductility of the cemented alloys. On the other hand, the high strengths in alloys such as WC-Co and TiC-Ni-Mo have been attributed to the thin matrix film, but no attempt has been made to analyze the systems on a quantitative basis.

The residual thermal stresses do play a part in the behavior of such cemented alloys, but there has been no simple correlation between these stresses and mechanical properties of such alloys.[7] These stresses are readily measured by X-ray diffraction analysis.

Lastly, assuming that during the deformation of such cemented alloys as in the W-Ni-Fe system the microscopic grains and matrix are in a state of triaxial stress, the effect of such a constraint must be considered. Unfortunately, there is no easy way of even qualitatively evaluating this effect.

"Delivered by Armour Research Foundation of Illinois Institute of Technology pursuant to Contract No. DA-11-022-505-ORD-3092. Government's use controlled by the provisions of Articles 26 and 27 of Title II (General Provisions)."

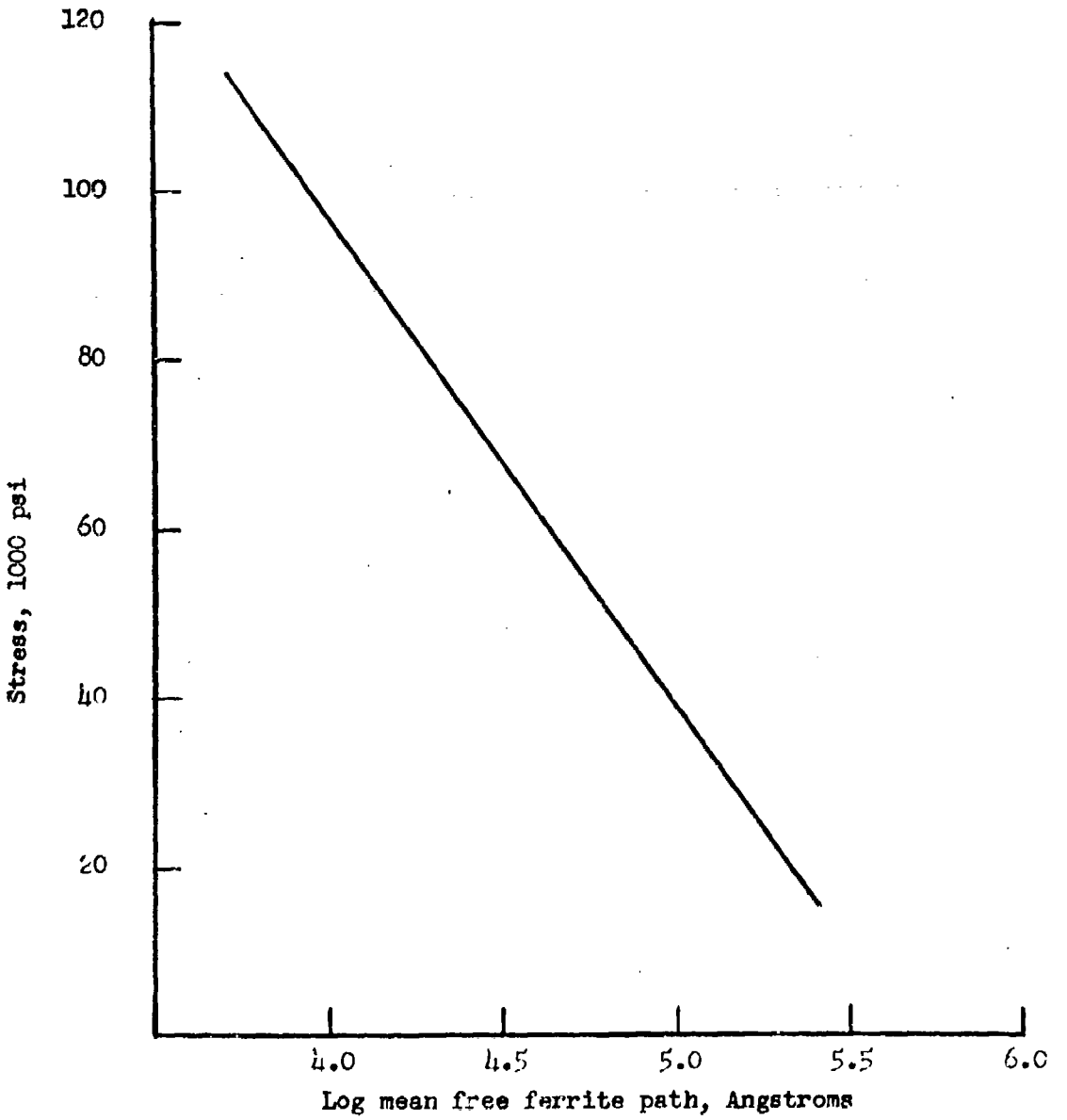

Fig. 1 Effect of the distance between cementite particles on the yield stress of the ferrite matrix (after Gensamer[6])

III. DEVELOPMENT OF THEORY

It is clear that the cemented alloys are quite different in their characteristics from the classical dispersion-hardened materials because the load-bearing capacity of the latter is derived from a critical dispersion of hard particles at such spacings as to offer the greatest resistance to propagation of slip. In the cemented alloys, however, the spacings between dispersed particles are too far apart to offer any appreciable resistance to slip propagation. Secondly, the dispersed phase is not really hard and brittle. And lastly we are trying to determine the sources of strength and ductility of such cemented alloys. Since the concept of dispersion hardening are not applicable to cemented alloys, a new approach is necessary to properly analyze the characteristic behavior of these alloys. A simple way of correlating the strength and ductility of cemented alloys (such as W-Ni-Fe) with the individual component properties would be to determine the strength-grain size relationship for the components. If A denotes the dispersed grains and B denotes the matrix, then the strength-grain size relationship for the components is given by

$$\sigma_y = \sigma_o + k_y d^{-1/2}$$

for both the components and

$$\sigma_F \propto d$$

where σ_y = yield strength

σ_F = fracture stress

σ_o = stress necessary to initiate motion of dislocations

d = grain diameter

and k_y = magnitude of the barrier opposing slip propagation.

"Delivered by Armour Research Foundation of Illinois Institute of Technology pursuant to Contract No. DA-11-022-505-ORD-3092. Government's use controlled by the provisions of Articles 26 and 27 of Title II (General Provisions)."

Let us plot σ vs d relationship for the hypothetical components A and B as in Fig. 2. Here we see that the σ_F and σ_y for A are both greater than those for B at all grain sizes. What is more important, the σ_F for B is less than σ_y for A. So in a cemented alloy of A and B, application of stress would result in fracture because σ_F - B is lower than σ_y - A and fracture would propagate through B. If, however, σ_F - A were lower than σ_y - B, the cemented alloy would be brittle and fracture would propagate through A. Thus, it appears reasonable that for ductile A - B cemented alloys the conditions to be fulfilled are:

$$\sigma_y - A \sim \sigma_y - B$$

$$\sigma_F - A \text{ and } \sigma_F - B > \sigma_y - A \text{ and } \sigma_y - B.$$

In the hypothetical case discussed above, this can be accomplished by manipulating the σ_o and k_y values for B by solid solution hardening or age hardening of the matrix B. It should be kept in mind that formation of any hard intermetallic compound in the cemented alloys would impart brittleness. Thus the grain-matrix interface in cemented alloys should be free of any barrier to propagation of slip. And slip would only propagate continuously if the flow stresses are reasonably well matched.

The basic tenet of the theory to be evaluated in the current program is that the strength and ductility of the cemented alloys in the W-Ni-Fe system are derived from the close matching of the flow stresses of the matrix and the dispersed tungsten grains. Since these flow stresses would have to be correlated in the size ranges of the components which are characteristic of the cemented alloys, a simple means of analyzing them would be to determine the yield strength-grain size relationships in the components and extrapolate them to the sizes of the components which are characteristic of the cemented alloys.

To accomplish this, it is essential to know the precise chemistry of the components in the sintered state. This can be accomplished by electron microprobe analysis of the components.

"Delivered by Armour Research Foundation of Illinois Institute of Technology pursuant to Contract No. DA-11-022-505-ORD-3092. Government's use controlled by the provisions of Articles 26 and 27 of Title II (General Provisions)."

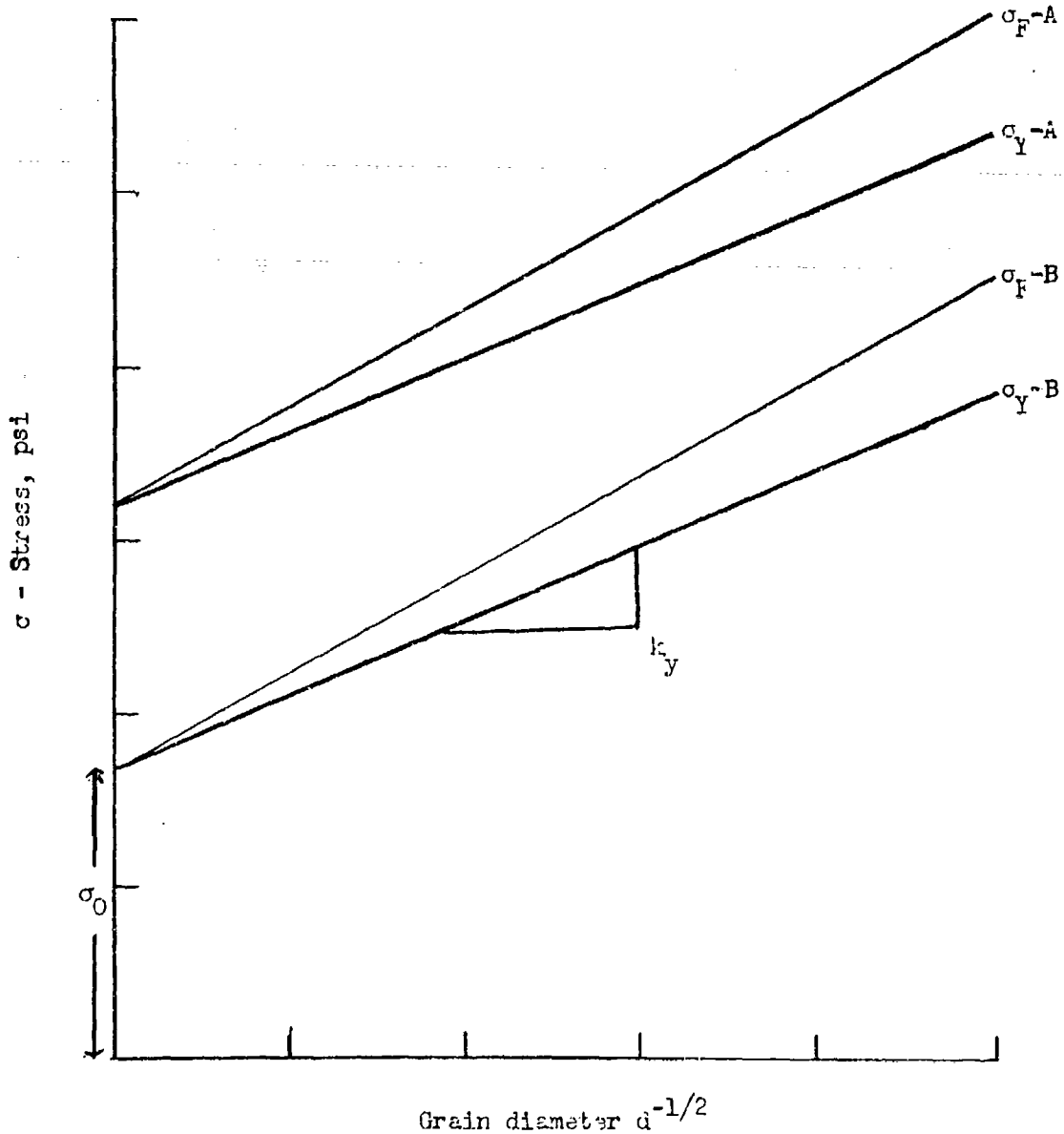

Fig. 2 Schematic representation of stress-grain size relationship in components of a cemented alloy. A -> grains; B -> Matrix

The significance of the principal residual thermal stresses should also be assessed. This can be accomplished by precise measurement of the changes in lattice parameters of the components with composition and calculating the stresses therefrom.

Besides all these factors, the importance of work-hardening characteristics of the components in the cemented structures cannot be ignored. These can be evaluated from the stress-strain curves.

The experimental results should give some idea of the relative importance of the various parameters discussed above in relation to the mechanical behavior of such cemented alloys.

IV. EXPERIMENTAL TECHNIQUES

A. Preparation of Sintered Bars

Sintered W-Ni-Fe bars were prepared by normal powder metallurgy techniques. The raw materials used were all powders of high purity. Tungsten powders of graded particle sizes were supplied by Sylvania, the nickel powder by International Nickel Co., and the iron powder by the National Radiator Co. The chemical analyses of the tungsten powders are summarized in Table I.

The required amounts of powders were weighed on a triple-beam balance and blended in glass jars for four hours on a ball mill rack. Transverse-rupture bars were pressed from these powders at about 6 tsi. The dimensions of the pressed bars were 2.00 in. x 0.25 in. x 0.15 in.

These bars were then placed in pure alumina trays (Morganite) and covered with high-purity alumina grit. The trays, which were 3 in. in diameter, were placed in a vacuum induction furnace which had a hot zone of 3 in. in diameter x 3 in. long. After the vacuum chamber was pumped down to about 50-micron pressure, the temperature of the heating chamber was increased to about 1450°C in one hour. Depending upon the tungsten content of the bars, the final sintering temperature ranged from 1435°C to 1530°C. This temperature

---

"Delivered by Armour Research Foundation of Illinois Institute of Technology pursuant to Contract No. DA-11-022-505-ORD-3092. Government's use controlled by the provisions of Articles 26 and 27 of Title II (General Provisions)."

TABLE I

CHEMISTRY OF TUNGSTEN POWDERS

Analysis	Tungsten Powder No.				
	I	II	III	IV	V
Average Particle Size, μ	1	3	5	7	9
Per cent Oxygen	0.11	0.08	0.05	0.03	0.03
Per cent Nonvolatiles	0.01	0.01	0.01	0.03	0.01
Per cent Molybdenum	0.0046	0.0017	0.001	0.001	0.001
Per cent Iron	0.001	0.001	0.001	0.001	0.001

"Delivered by Armour Research Foundation of Illinois Institute of Technology pursuant to Contract No. DA-11-022-505-ORD-3092. Government's use controlled by the provisions of Articles 26 and 27 of Title II (General Provisions)."

was maintained for one hour, and then the power was turned off. The samples cooled down to a few hundred degrees in about two hours. They were then unloaded and finished for testing.

B. Processing of Matrix Alloy

Several steps were involved in preparation and processing the matrix alloy. The raw materials used were Armco ingot iron, electrolytic nickel, and ferrotungsten. These materials, in the right proportions, were arc melted in an Argon arc furnace in order to obtain 3 in. diameter buttons weighing about 400 gm. These buttons were impossible to cold work due to their chilled microstructure, so they were vacuum melted in an alumina crucible and furnace cooled. This slow cooling improved their microstructure considerably. The buttons thus produced were surface ground to obtain flat discs, which were then cold rolled to various reductions and recrystallized at 1600° to 1650°F for different times. Thus it was possible to obtain test bars (2.00 in. x 0.25 in. x 0.125 in.) with varying grain sizes from ASTM-1 to ASTM-8.

C. Processing of Pure Tungsten Bars

Pure tungsten strips were obtained from Fansteel Metallurgical Corp. These were of the X-ray target grades. The strips were cut to the transverse-rupture bar size and warm rolled at 550°C in air from 15 to 30 per cent reduction. These were then recrystallized at 1950°C to 2100°C in vacuum from 1 to 3 hours. The bars thus processed had uniform grain size in a range of ASTM-4 to ASTM-8. Production of larger grain sizes would have entailed a detailed investigation of recrystallization behavior of pure tungsten, which was outside the scope of the current program.

D. Mechanical Property Measurement

All the mechanical property measurements were made using transverse rupture bars. Most of the room-temperature measurements were performed on a Hounsfield Tensometer using a three-point loading device. The elevated temperature (up to 1200°F) testing was done on the "Instron" Universal tester with a four-point loading device. In both cases the sample sizes were main-

"Delivered by Armour Research Foundation of Illinois Institute of Technology pursuant to Contract No. DA-11-022-505-ORD-3092. Government's use controlled by the provisions of Articles 26 and 27 of Title 11 (General Provisions)."

tained close to the uniform dimension of 1.75 in. x 0.25 in. x 0.125 in. Due to the nature of the tests, the elongations cannot be reported in conventional terms; only the deflections are reported. However, by experience it was found that for alloys in this system a deflection of 0.25 in. corresponded to cold rollability of about 60 per cent.

E. Metallography and Microhardness

The faces of the samples to be examined were mounted in bakelite and polished on an automatic polishing wheel through 120, 240 and 400 grit emery paper. Deep scratches were then removed by using a 9-micron diamond paste on a felt. Final polish was then given to the samples by using Al_2O_3 Linde "A" suspension in water, again on the automatic polisher.

The etching of the matrix alloy was accomplished with a dilute solution of alkaline ferricyanide. The tungsten grains in pure tungsten were also etched with the same solution.

Microhardness measurements were made on a Leitz microhardness tester using a Vickers indenter. The load was kept uniformly at 15 gm for all samples to produce small impressions. Larger impressions gave erroneous results due to the small sizes of the matrix alloy and tungsten grains in the cemented structures.

F. Electron Microprobe Analysis

In the technique of electron microprobe analysis, an electron beam focused to a diameter of about one micron is allowed to bombard the region of a polished specimen from which a chemical analysis is desired. The interaction between the electron beam and the specimen results in the production of the characteristic X-rays of the elements present in the bombarded region. Since the depth of penetration of the electrons is approximately one micron, the resulting X-rays originate within a few millionths of a microgram of material. An analysis of this X-ray spectrum from the region of unknown

---

"Delivered by Armour Research Foundation of Illinois Institute of Technology pursuant to Contract No. DA-11-022-505-ORD-3092. Government's use controlled by the provisions of Articles 26 and 27 of Title II (General Provisions)."

chemical composition is obtained with the aid of an X-ray spectrograph and compared with the spectrum from specimens of known chemical composition. The machine used in the present investigation is owned by the Research Laboratories of International Nickel Co., Bayonne, New Jersey, and employs a flow counter in addition to a proportional counter for analyzing the X-ray spectrum. The electron beam in this equipment could be focused down to a one micron diameter spot on the specimen surface, and the intensity and location of the spot could be retained without drift for long periods of time. The counters had an accuracy of measurement of about 0.1 per cent. The lateral motion of the specimen was made possible in two directions by a micrometer stage which was free of backlash. The electron beam was perfectly aligned with the optical axis of the microscope, and the bombarded spot could be easily seen because of localized deposition of the decomposition products of the diffusion pump oil present in the system. The use of the flow counter made it possible to analyze for light elements down to magnesium in the periodic table.

G. Residual Stresses by the X-ray Method

Residual thermal stresses in the cemented alloys were calculated from the precise measurements of the changes in lattice parameters of the components with changes in composition.

Lattice parameter changes in the matrix alloys were calculated from the averages of two reflections, hkl = 311 and 222. All the measurements were performed on a Norelco Diffractometer using iron radiation at 40 KV and 10 ma.

Previous Debye-Scherrer photographs of these samples indicated that the back-reflection lines were broadened enough so that the α_1 α_2 components of the characteristic Fe K_α radiation were not resolved. This line broadening was undoubtedly due to small crystallite size, lattice strains, etc. In order to obtain accurate measurements, it is imperative to have samples of optimum crystal size in the unstrained condition. However, this problem was overcome by scanning and manually counting the angular range over which the reflections occur. The counting intervals were 0.1 to 0.2° 2θ. The counts per second were then plotted against the angle 2θ . The resulting curves represented the combined effects of Fe K_{α_1} and K_{α_2}. Because of the broadness and

"Delivered by Armour Research Foundation of Illinois Institute of Technology pursuant to Contract No. DA-11-022-505-ORD-3092. Government's use controlled by the provisions of Articles 26 and 27 of Title II (General Provisions)."

asymmetry of the curves, the peak 2θ values would not be valid. To obtain corrected $2\bar{\theta}$ values, the center of gravity of each curve was calculated. From this corrected $2\bar{\theta}$ and the weighted Fe K_α wavelength, the d values and subsequently the a_o values were calculated.

$$\text{corrected } 2\bar{\theta} = \frac{2\theta\, I\,(2\theta)}{I\,(2\theta)}$$

$$\text{weighted Fe } K_\alpha = \frac{2\lambda K_{\alpha 1} + \lambda K_{\alpha 2}}{3}$$

$$d = \frac{\lambda/2}{\sin \bar{\theta}}$$

$$a = d\sqrt{h^2 + k^2 + l^2}$$

To illustrate the difficulty in measuring the peak 2θ value, the hkl reflections of the matrix alloy in the cemented structure exhibited intensities of only about 5 counts per second greater than the background radiation.

Measurements were made on the as-sintered samples, polished samples, and etched samples.

V. RESULTS

A. Processing Variables in Sintered Compositions

The basis of preparation of sintered W-Ni-Fe alloys was liquid-phase sintering. In this technique, a powder compact of this alloy is heated in vacuum or hydrogen at a temperature above the melting point of the nickel-rich alloy. The densification takes place by solution and reprecipitation of tungsten grains in the liquid. To establish the optimum processing conditions, a single composition, 90W-10(7Ni-3Fe), was selected for investigating the effect of sintering temperature and time and influence of initial particle size of tungsten.

"Delivered by Armour Research Foundation of Illinois Institute of Technology pursuant to Contract No. DA-11-022-505-ORD-3092. Government's use controlled by the provisions of Articles 26 and 27 of Title II (General Provisions)."

1. Sintering Time and Temperature

The influence of sintering time and temperature on the yield strength of the 90W-10(7Ni-3Fe) alloys is plotted in Fig. 3. All these alloys were sintered to full density. It can be seen that the alloys sintered at temperatures below 1440°C have poor yield strengths. This is due to the fact that the samples sintered at 1350°C and 1400°C were densified only in the solid state and exhibit a highly segregated microstructure. Also, at these temperatures there is no appreciable solution of tungsten in the nickel-rich matrix -- thereby resulting in a weak matrix. Figure 4a and 4b show, respectively, the above-mentioned alloy sintered at 1350°C and 1475°C, respectively --the former representing the "undersintered" microstructure and the latter a good "liquid-phase sintered" microstructure. From these results it was apparent that one hour at temperature was sufficient for good samples. Excessive time or temperature of sintering above the melting point of the matrix resulted in loss of matrix by evaporation or migration of the matrix to the surface of the samples. The microstructures of these alloys indicate that almost all the grain growth of tungsten is completed within the first 15 minutes of sintering although the elimination of voids takes about one-half hour at 1440°C and above.

2. Initial Particle Size of Tungsten

The effect of the initial particle size of tungsten on the yield strength of liquid-phase sintered alloy of composition 90W-10(7Ni-3Fe) was also investigated. The results are plotted in Fig. 5. It was found that alloys with larger initial particle size of tungsten were a little weaker and slightly porous. The optimum particle size of about 3 microns was selected as a standard for the remainder of the program.

3. Tungsten Content

Due to the nature of the sintering process, the sintering time and temperature were expected to be different for different concentrations of tungsten. Series of tests were made to establish the optimum sintering

---

"Delivered by Armour Research Foundation of Illinois Institute of Technology pursuant to Contract No. DA-11-022-505-ORD-3092. Government's use controlled by the provicions of Articles 26 and 27 of Title II (General Provisions)."

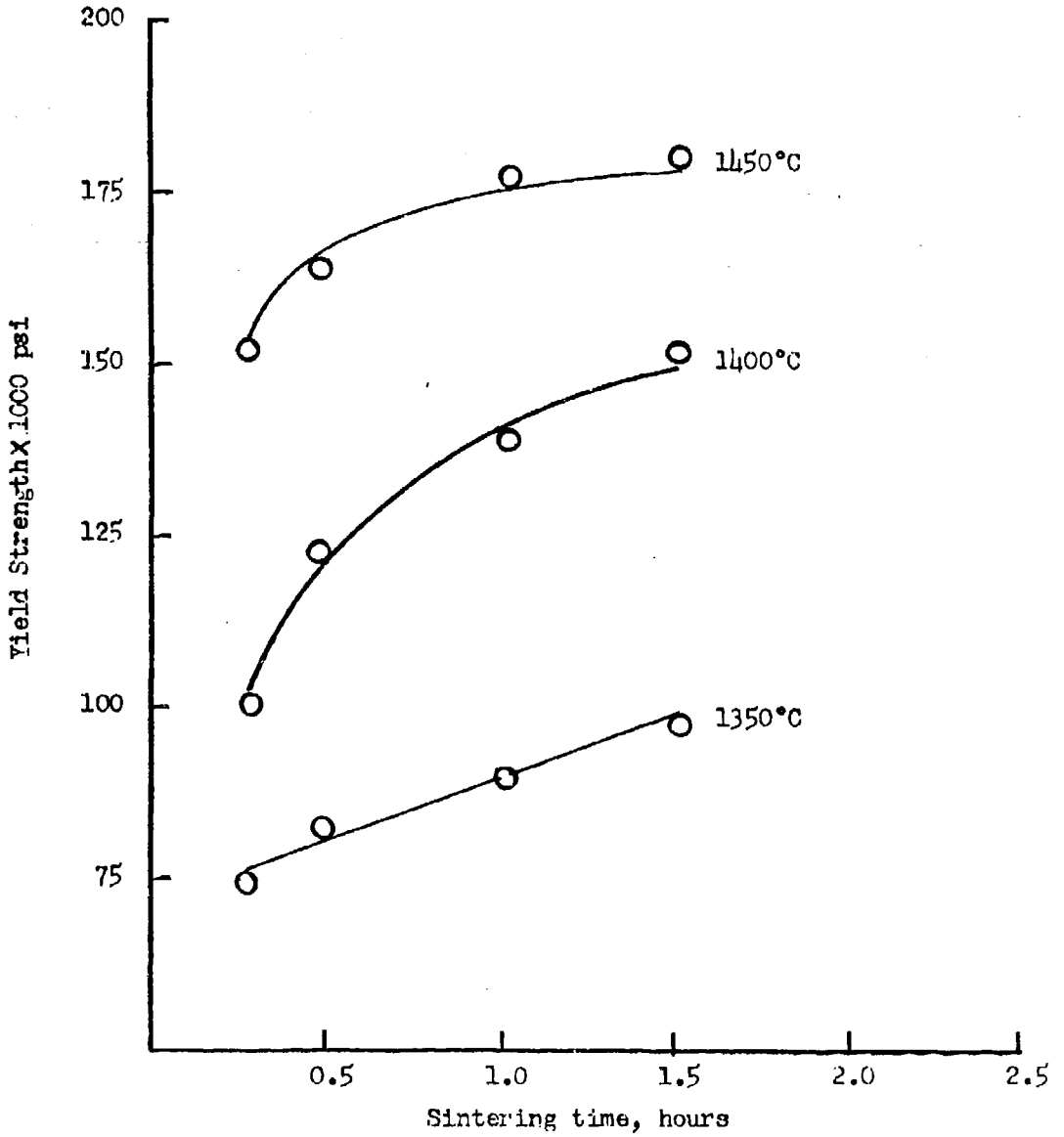

Fig. 3 Influence of sintering time and temperature on yield strength of 90W-10(7Ni-3Fe) alloys. Hounsfield Tensometer tests. Three-point loading.

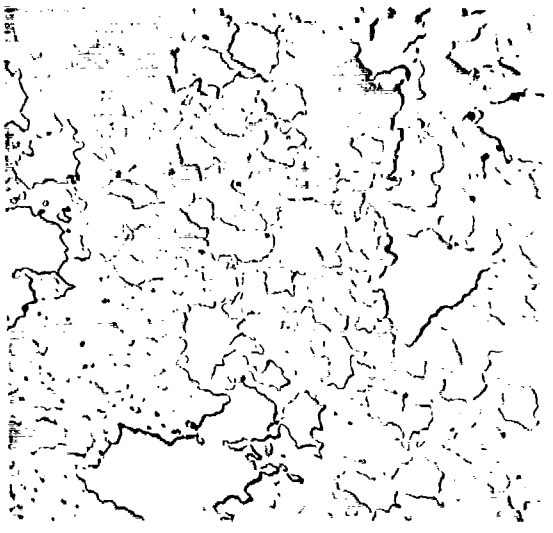

500X

Fig. 4(a) Neg. 19897

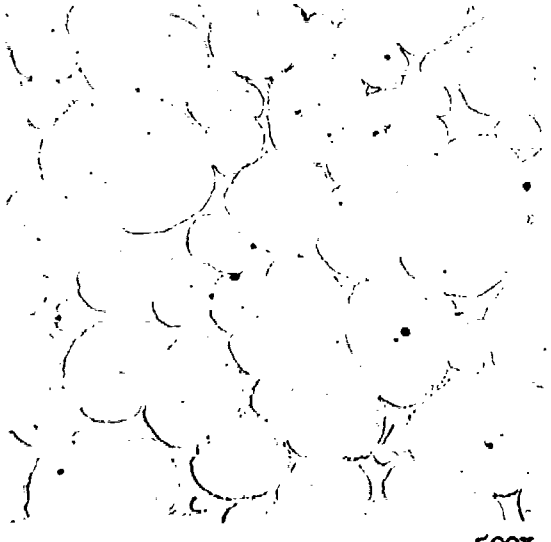

500X

Fig. 4(b) Neg. 19900

Fig. 4(a) Microstructure of 90W-10(7Ni-3Fe) sintered at 1350°C - 1 hour - vacuum. Note "undersintered" structure.

Fig. 4(b) Microstructure of 90W-10(7Ni-3Fe) sintered at 1475°C - 1 hour - vacuum. Liquid-phase sintered structure.

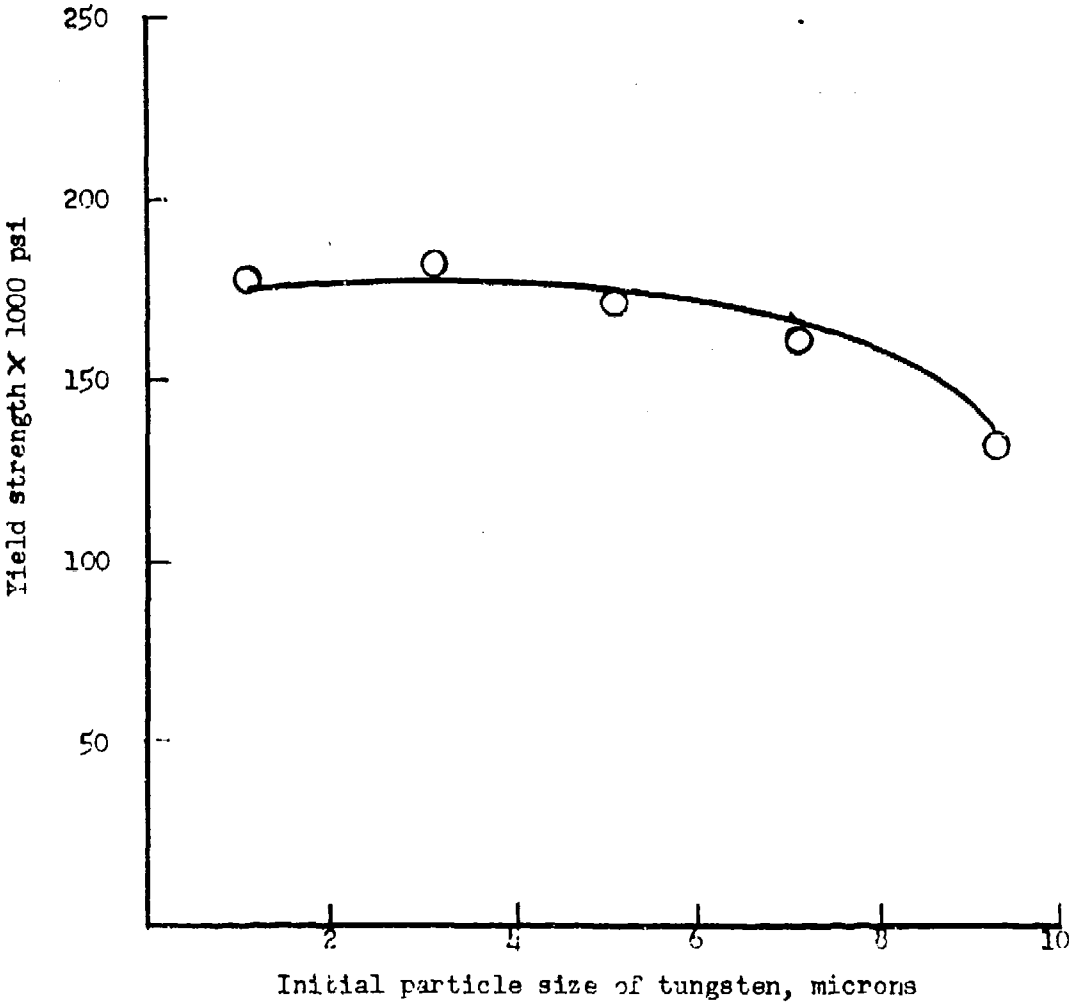

Fig. 5 Effect of initial particle size of tungsten on yield strength of 90W-10(7Ni-3Fe) alloys sintered at 1475°C - 1 hour - vacuum. Hounsfield sintered at 1475°C - 1 hour - vacuum. Tensometer tests. Three-point loading.

temperatures for one hour of sintering time for compositions containing 75 to 95 per cent tungsten and balance nickel and iron in a ratio of 7:3. The results are plotted in Fig. 6.

B. Properties of Sintered Compositions

1. Influence of Tungsten Content

The effect of tungsten content on the yield strength of the sintered bars is reproduced in Fig. 7. The measurements were made on the Hounsfield Tensometer using a three-point loading device. It may be noted that samples containing less than 80 per cent tungsten show low yield strengths and a great deal of scatter. This is because it is impossible to avoid gross segregation of tungsten in these alloys. Although the data reported in Fig. 7 refer to measurements made on alloys with a nickel-iron ratio of 7:3, changing this ratio to 6:4 does not alter the picture measurably.

The influence of tungsten content on the total deflection of the sintered bars is also plotted in Fig. 7. The deflection is fairly constant until high tungsten contents are reached, whereupon it begins to drop -- most probably because the alloys with high tungsten content begin to exhibit properties similar to those of pure tungsten due to the continuity of the tungsten grains.

2. Temperature Dependence of Yield Strength of Sintered Alloys

Yield strengths of sintered alloys containing varying percentages of tungsten were measured in the Instron Universal tester using a four-point loading device. The results are reproduced in Fig. 8. For the bars containing less than 90 per cent tungsten, the strength drops evenly with increasing temperatures. However, for the higher tungsten bars, there seems to be no further drop after 400°F up to 1200°F. This may be due, again, to the fact that, for alloys with high tungsten contents, there is very little matrix and we may well be measuring the yield strength of pure tungsten. These tests were all performed in air.

"Delivered by Armour Research Foundation of Illinois Institute of Technology pursuant to Contract No. DA-11-022-505-ORD-3092. Government's use controlled by the provisions of Articles 26 and 27 of Title II (General Provisions)."

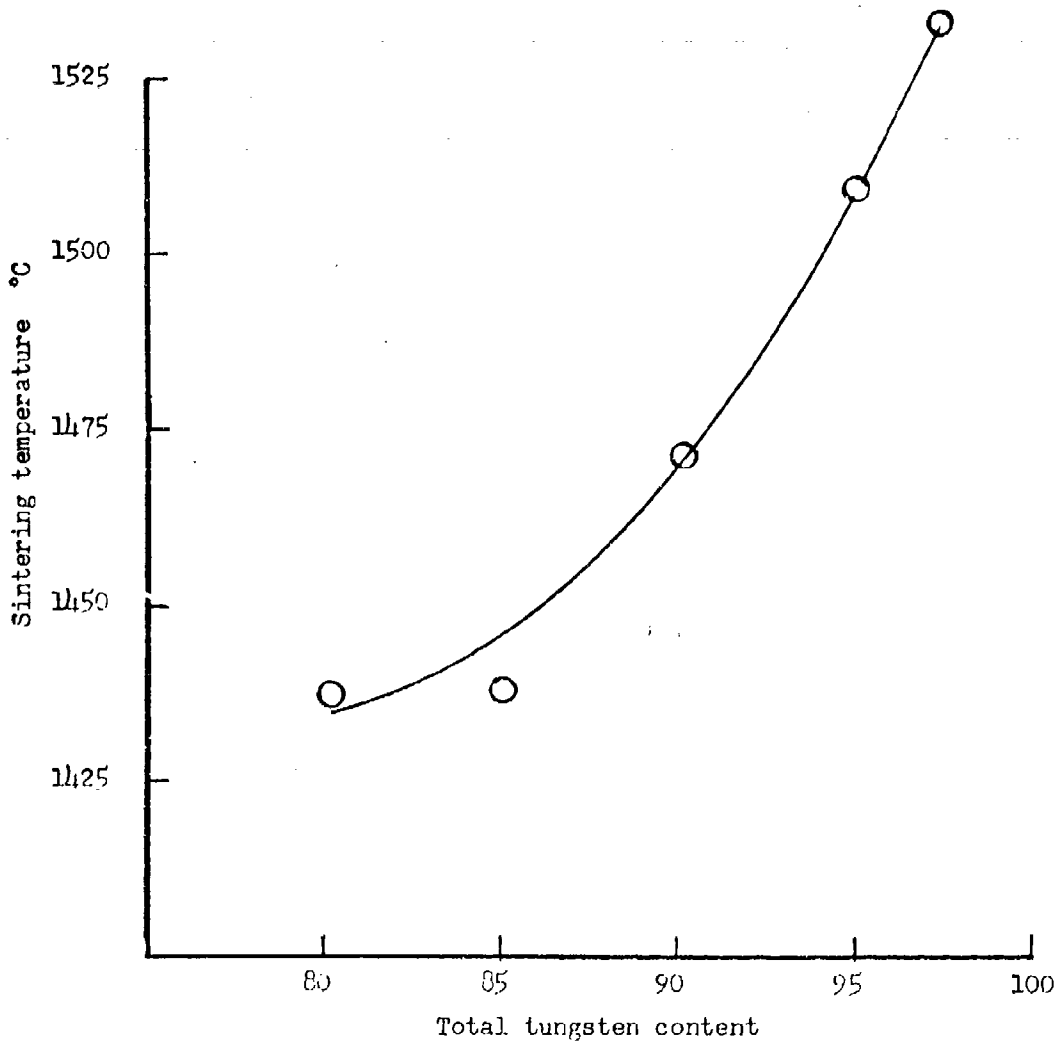

Fig. 6 Optimum sintering temperature for one hour of sintering time for alloys of various tungsten contents and nickel to iron ratio of 7:3.

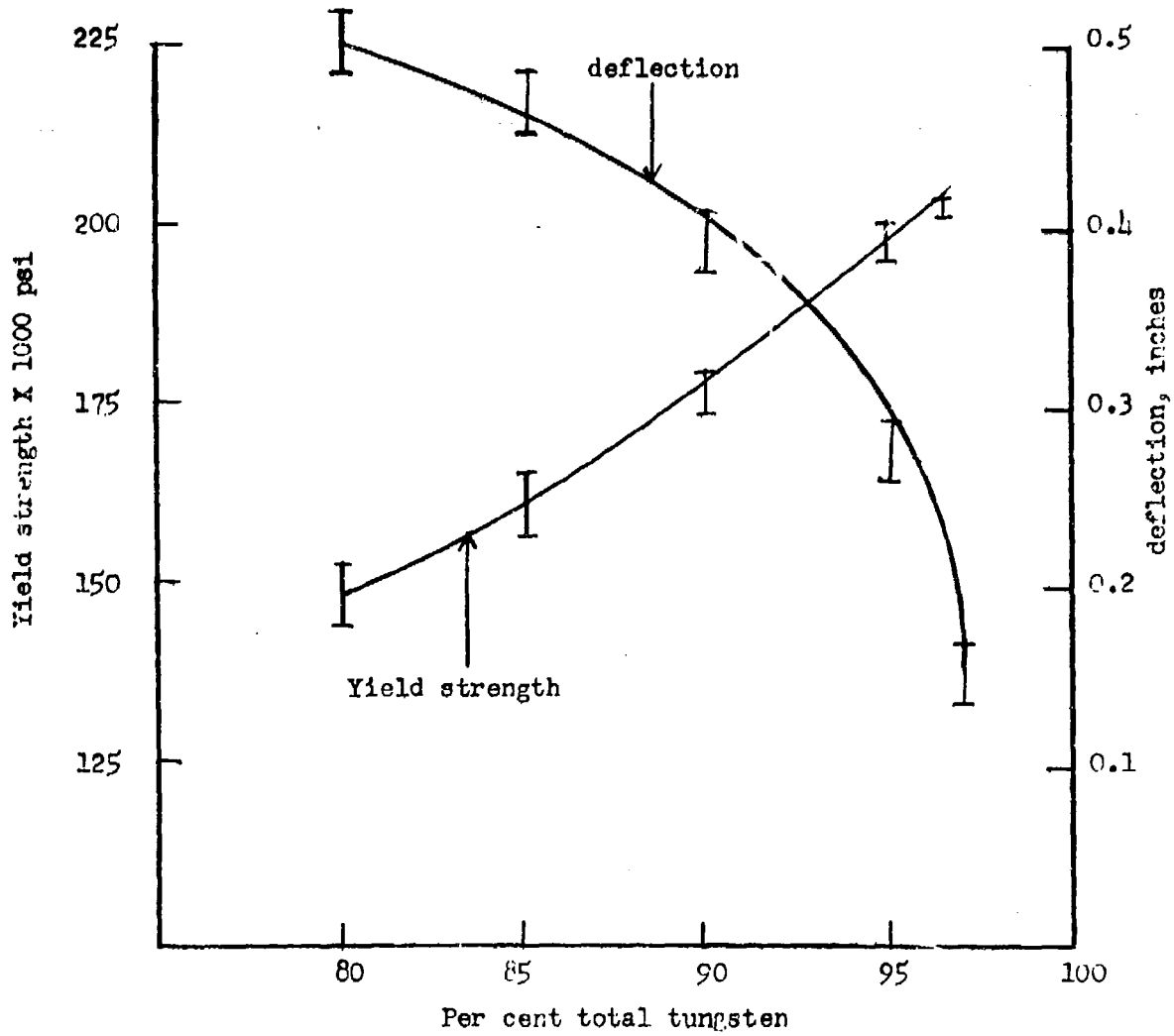

Fig. 7 Effect of tungsten content on yield strength and deflection of cemented W-Ni-Fe alloys with nickel to iron ratio of 7:3. Hounsfield Tensometer tests. Three-point loading.

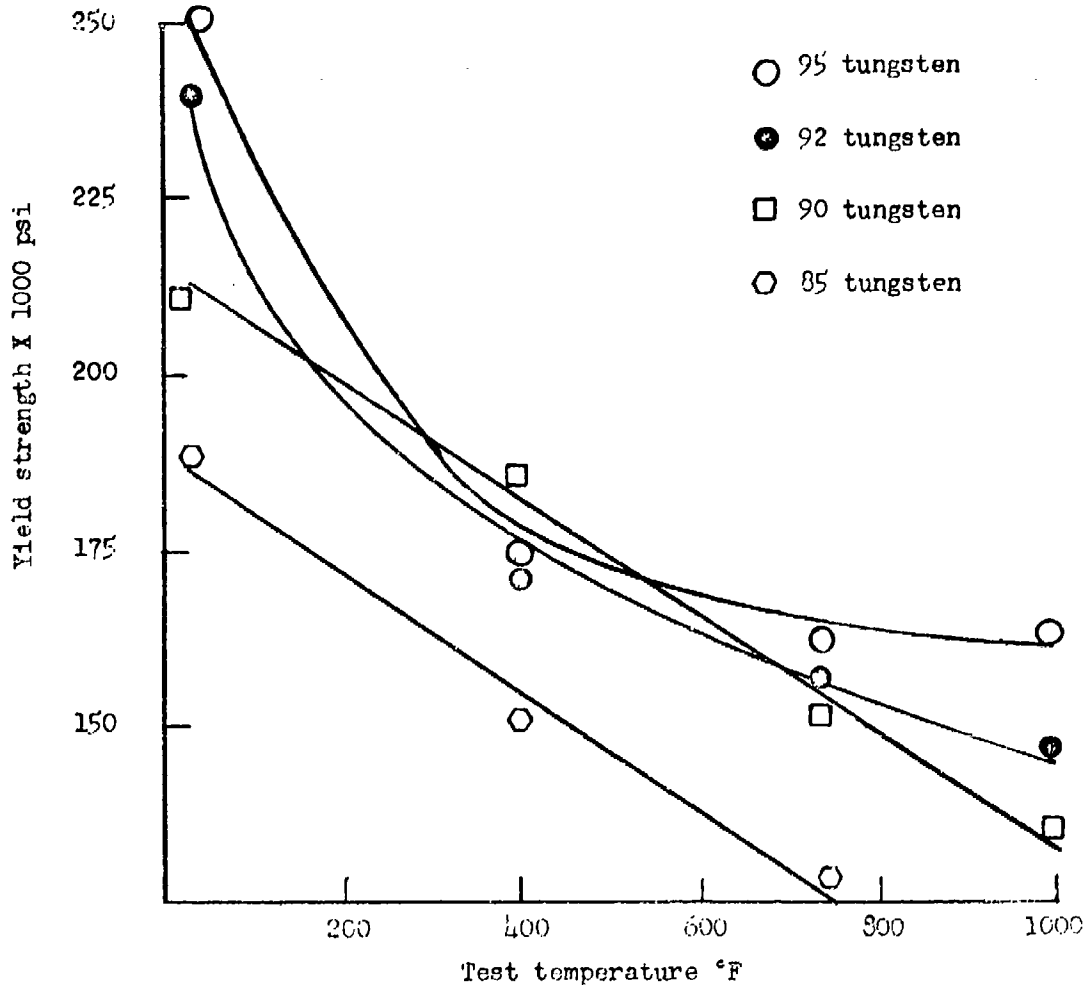

Fig. 8 Temperature dependence of yield strength of cemented W-Ni-Fe alloys with nickel to iron ratio of 7:3. Instron tests. Four-point loading.

3. Temperature Dependence of Deflection of Sintered Alloys

The effect of temperature on the deflection of sintered alloys is plotted in Fig. 9. It can be seen that there is no measurable change in deflection with temperature of alloys containing less than 90 per cent tungsten. However, the alloys with higher tungsten content actually exhibit an increase in deflection (or ductility) with increasing temperatures. This phenomenon again corroborates the view that properties of high-tungsten alloys (> 90 per cent) are determined by properties of tungsten, and the increase in deflection can be explained by the fact that, with increasing temperatures, the brittle-ductile transition zone of tungsten is entered upon. In the initial experiments the limit of deflection of these bars on the Instron was 0.3 inch due to the geometry of the knife edges. The knife edges were later modified for measuring higher deflections. However, the results are unambiguous and reproducible. It may be recalled that for alloys in this system a deflection of about 0.25 inch corresponds to cold rollability of about 50 - 60 per cent.

4. Discontinuous Yield in High-Tungsten Bars

It was observed that samples with greater than 90 per cent tungsten exhibited a discontinuous yield, the magnitude of which increased with increasing temperature. The results are reproduced schematically in Fig. 10.

C. Matrix Alloy

According to the concepts outlined in Section III and procedures described in Section IV, the grain size dependence of yield strength of the matrix alloy was measured in the Instron tester. The electron microprobe analysis of the matrix alloy showed a composition of 24W-76(7Ni-3Fe). However, arc-cast and vacuum-melted ingots of this alloy were almost impossible to cold work more than 15 per cent without cracking. The alloy buttons which were cold worked less than 15 per cent recrystallized only to large grain sizes. This problem was overcome by dropping the tungsten content of the single-phase matrix alloy to 18 and 15 and measuring the yield strength-grain size relationship in these alloys. These results, combined with the same

"Delivered by Armour Research Foundation of Illinois Institute of Technology pursuant to Contract No. DA-11-022-505-ORD-3092. Government's use controlled by the provisions of Articles 26 and 27 of Title II (General Provisions)."

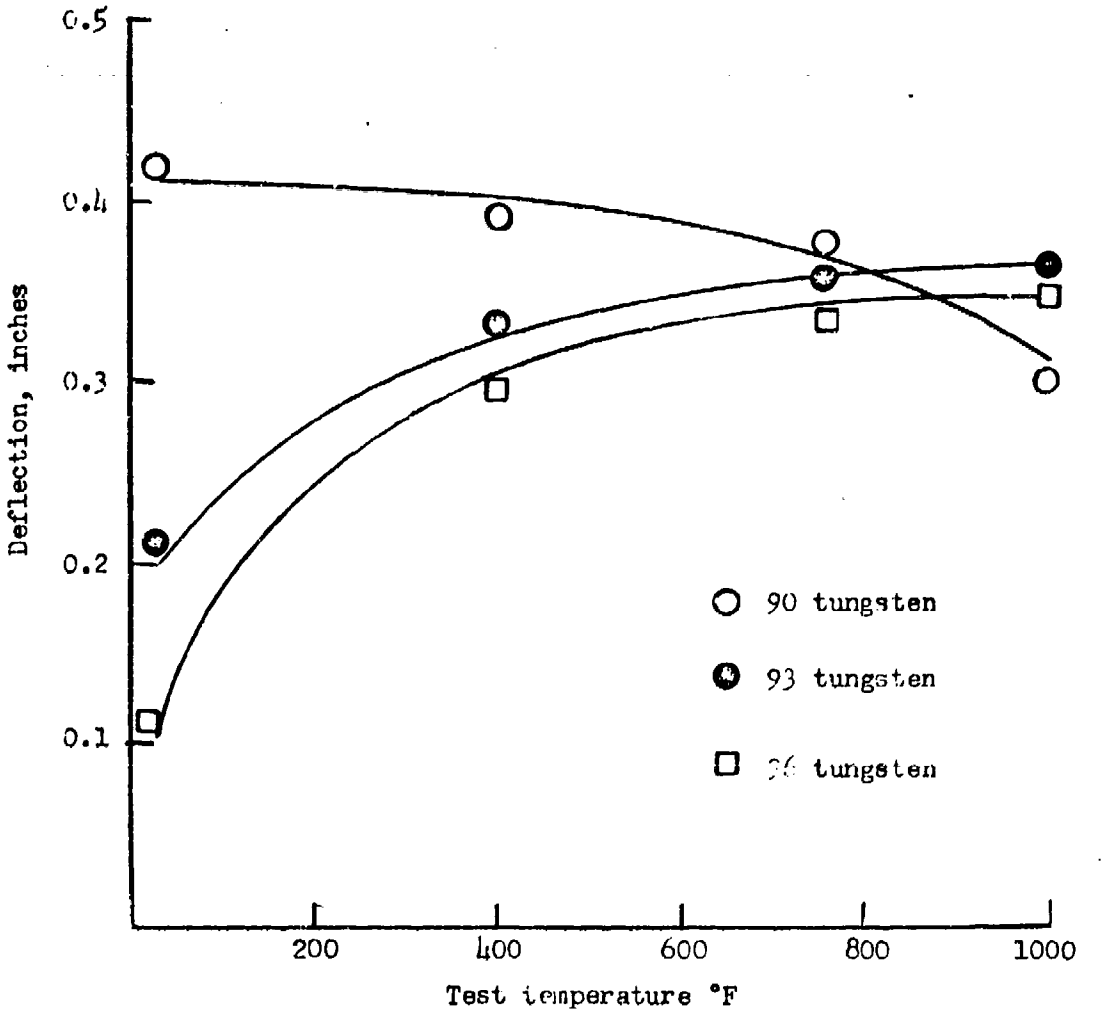

Fig. 9 Temperature dependence of deflection of cemented W-Ni-Fe alloys with nickel to iron ratio of 7:3. Instron tests. Four-point loading.

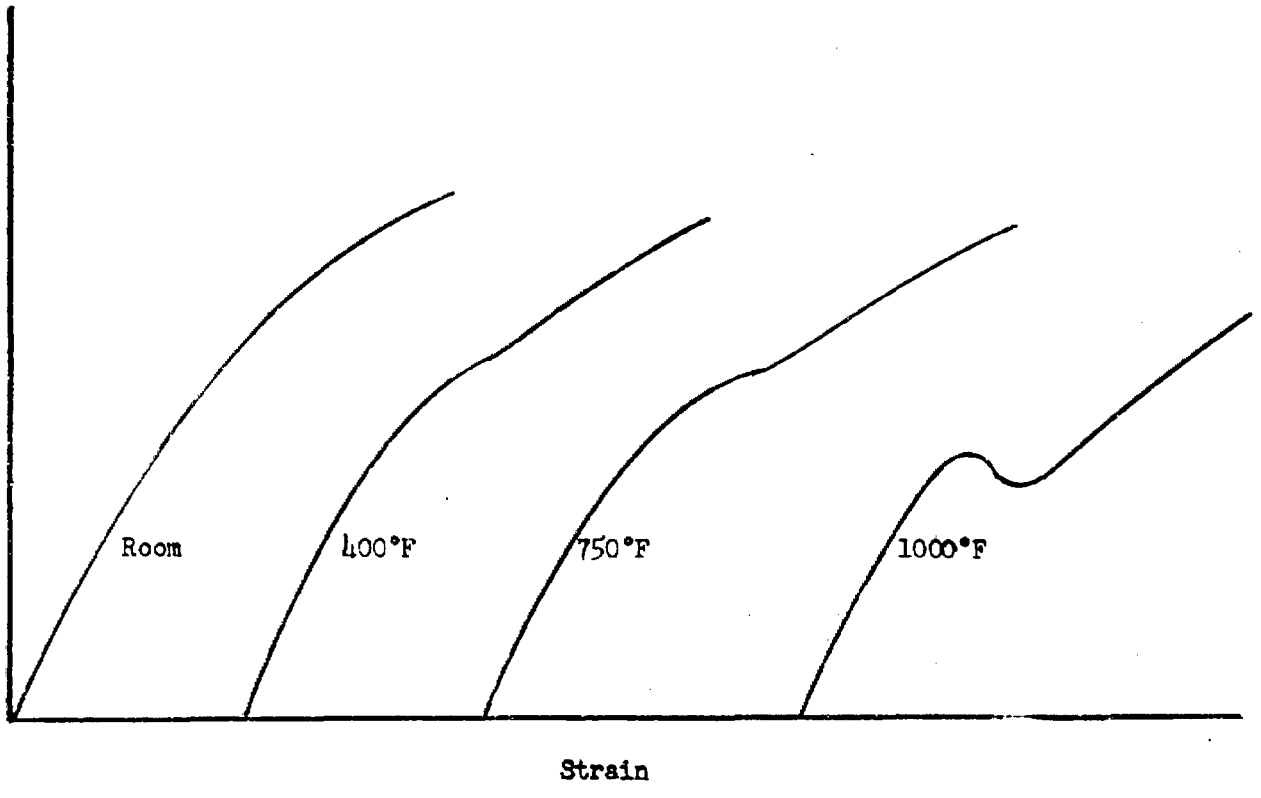

Fig. 10 Discontinuous yield in 95W-5(7Ni-3Fe) alloys at various temperatures. Schematic representation of stress-strain curves. Instron tests. Four-point loading.

relationship for large grain sizes for the matrix alloy containing 24W, enabled the results for the matrix alloy of 24W-76(7Ni-3Fe) to be extrapolated with confidence. The room-temperature grain size dependence of yield strength for matrix alloys of three different tungsten contents is plotted in Fig. 11. Extrapolation of the plot for 24W-76(7Ni-3Fe) provide a value for the yield strength of this alloy at a grain size comparable to that found in the cemented structure (i.e., the matrix film thickness).

A comparative study, the same relationship was determined for a binary Ni-28W alloy and also for copper. The results are plotted in Fig. 12 and will be discussed later.

The temperature dependence of the yield strength - grain size relationship in the matrix alloy of composition 24W-76(7Ni-3Fe) was investigated and is plotted in Fig. 13.

During the investigation of the recrystallization characteristics of the matrix alloy, a systematic study was made of the properties of the cold-worked alloy. The effect of degree of cold work on the strength and microhardness of the matrix alloy of composition 18W-82(7Ni-3Fe) is plotted in Fig. 14.

D. Pure Tungsten

Commercially pure tungsten strips were obtained from Fansteel Metallurgical Corporation. These strips were warm worked at about 550°C and recrystallized at various times from 1950°C to 2100°C in vacuum. It was difficult to obtain a very wide range of grain sizes for pure tungsten and especially difficult to grow grains of sizes larger than ASTM-4. The temperature and grain size dependence of yield strength for pure tungsten is plotted in Fig. 15. If these results are compared with those reported for the matrix alloy in Fig. 13, a close matching of the respective yield strengths of the two materials is found for the grain sizes which are characteristic of the cemented structures.

"Delivered by Armour Research Foundation of Illinois Institute of Technology pursuant to Contract No. DA-11-022-505-ORD-3092. Government's use controlled by the provisions of Articles 26 and 27 of Title II (General Provisions)."

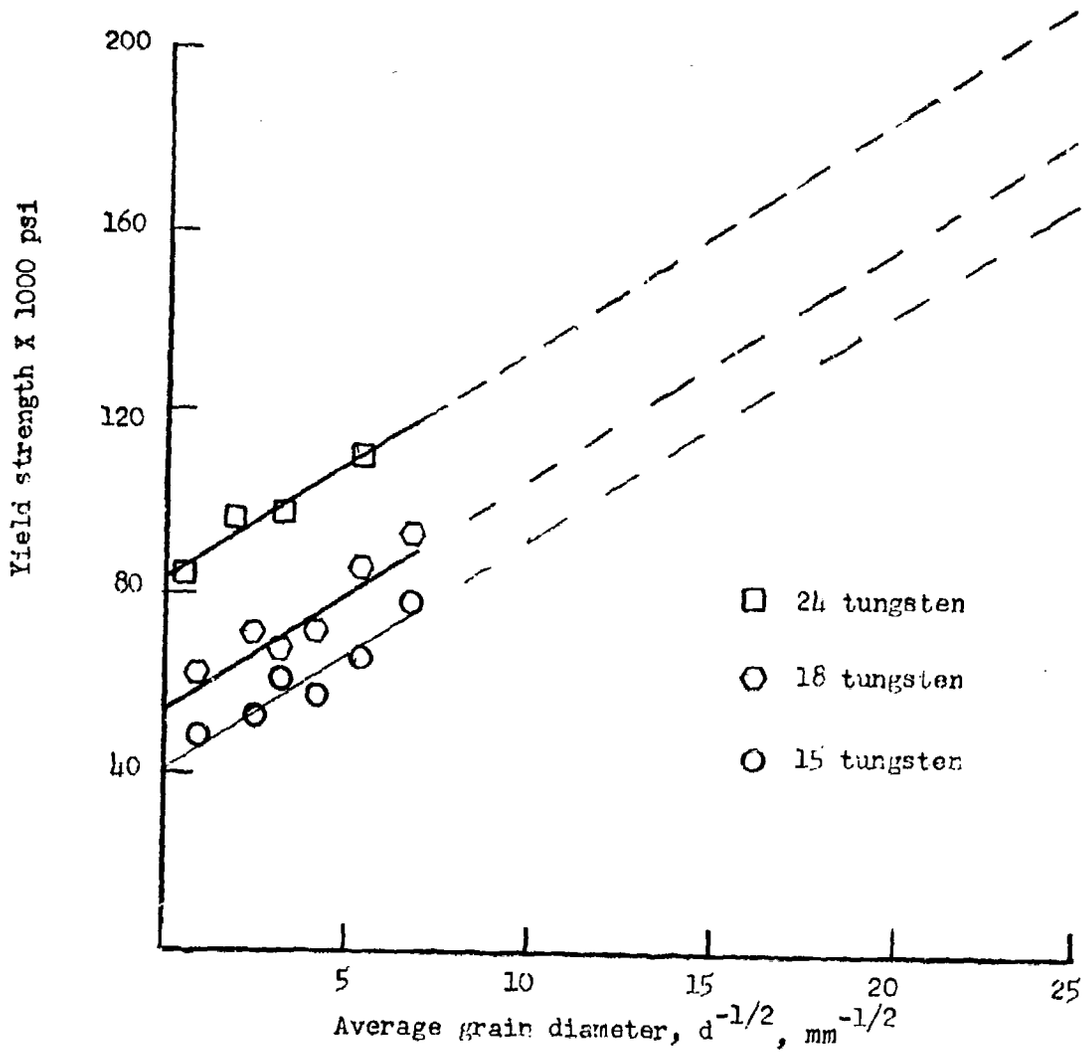

Fig. 11 Grain size dependence of yield strength of single phase matrix alloys of different tungsten contents and nickel to iron ratio of 7:3. Hounsfield Tensometer tests. Three-point loading.

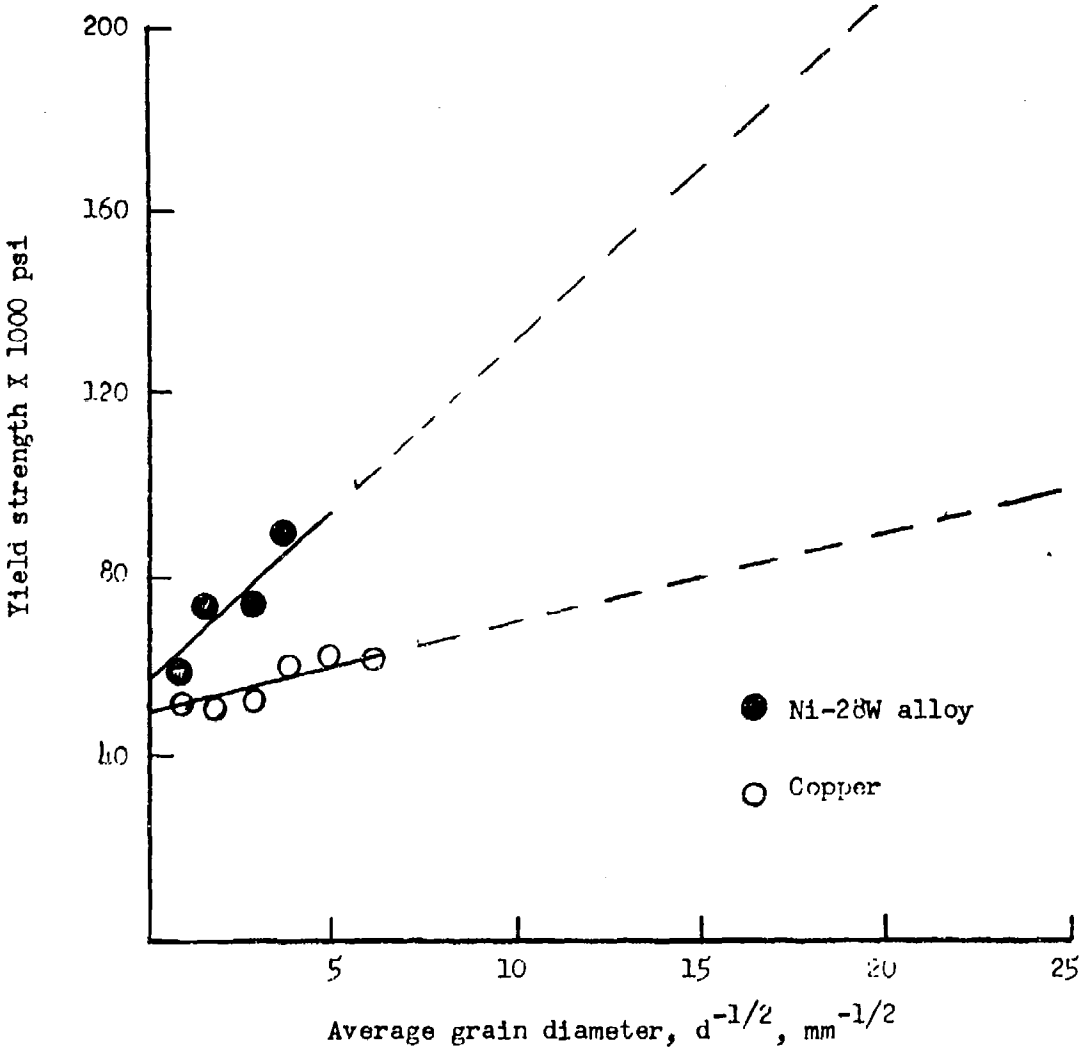

Fig. 12 Grain size dependence of yield strength of single phase Ni-28W alloy and copper. Hounsfield Tensometer tests. Three-point loading.

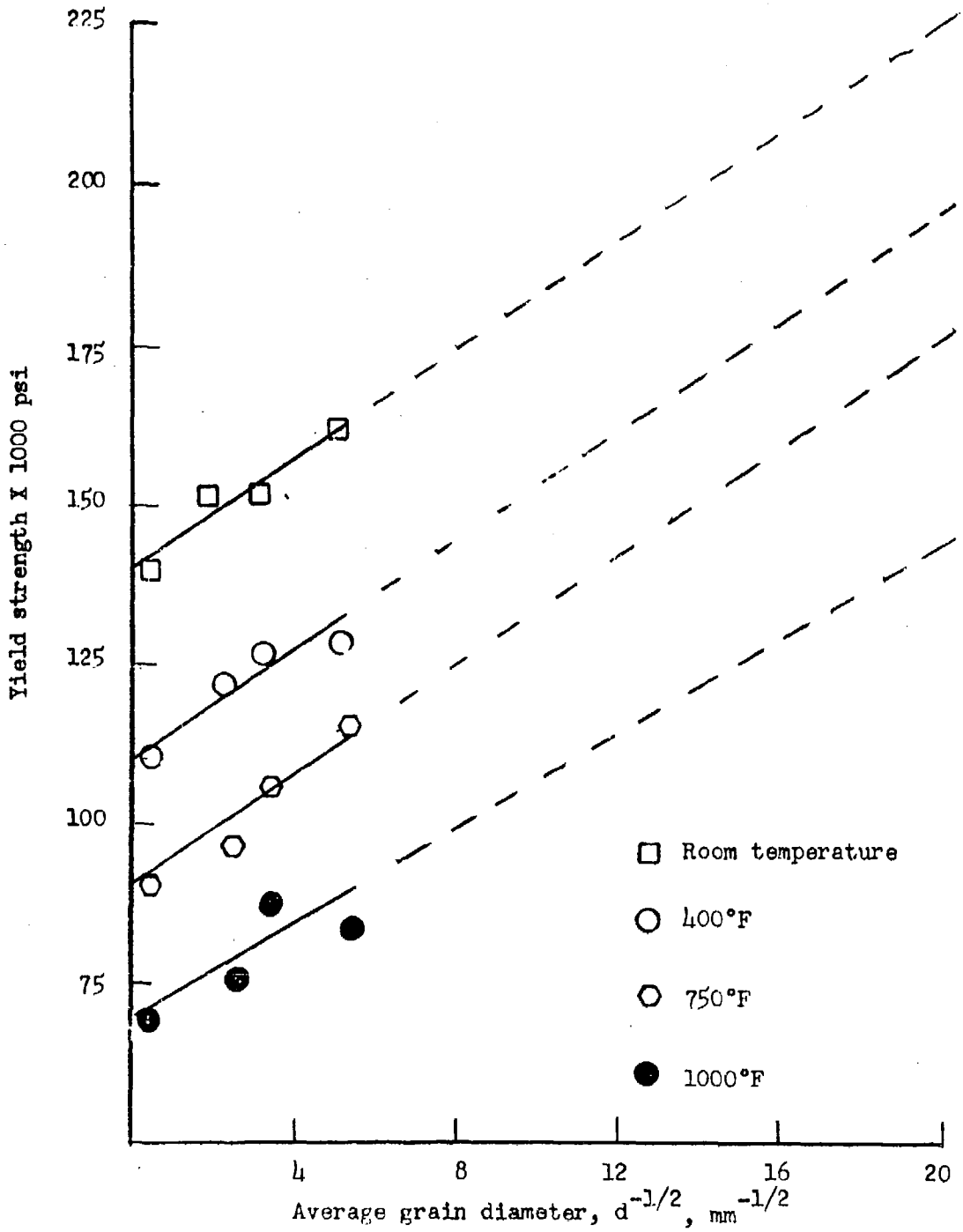

Fig. 13 Temperature dependence of yield strength-grain size relationship of matrix alloy of composition 24W-76(7Ni-3Fe). Instron tests. Four-point loading.

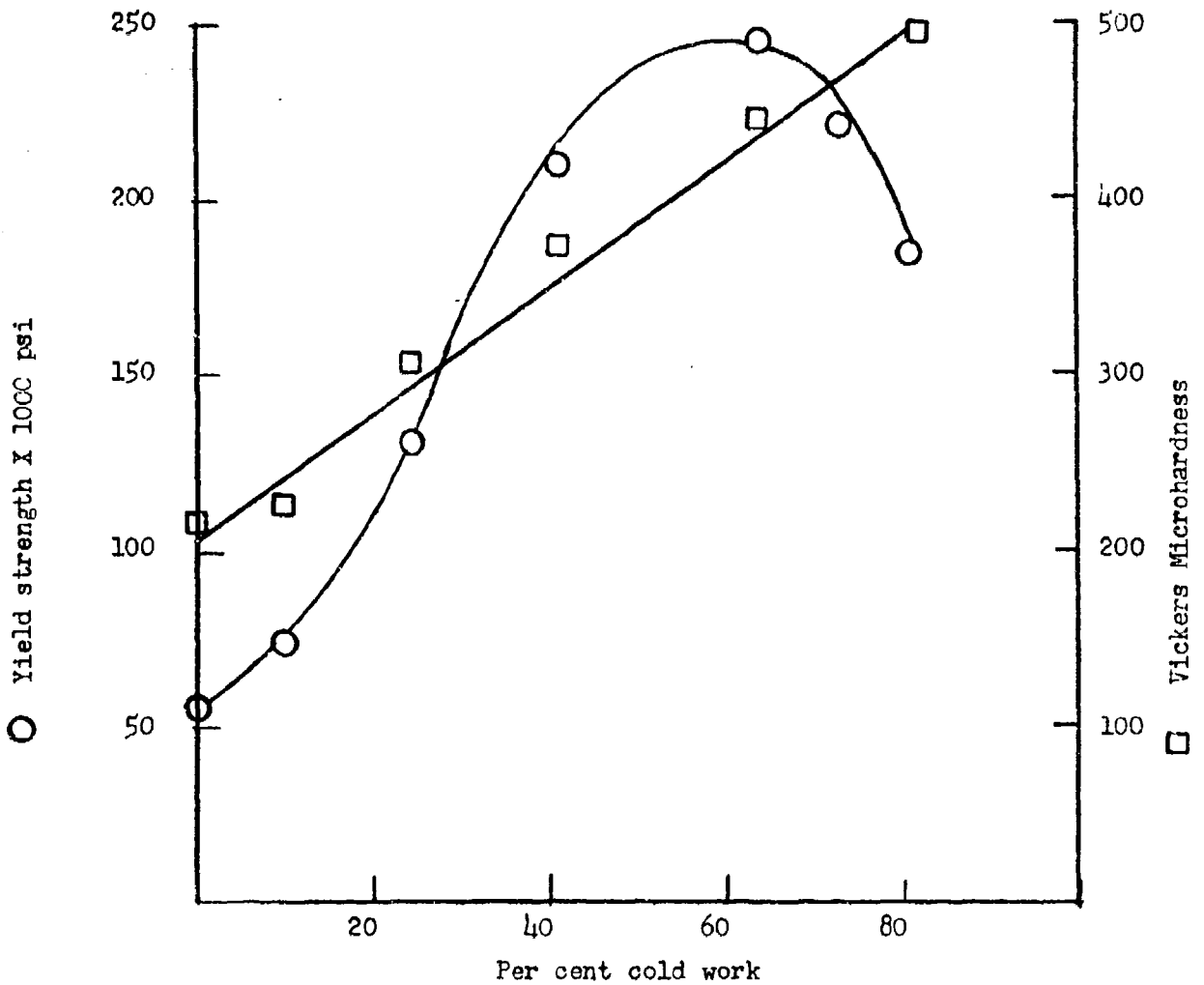

Fig. 14 Effect of cold work on yield strength and microhardness of single phase matrix alloy of composition 18W-82(7Ni-3Fe). Hounsfield Tensometer tests. Three-point loading.

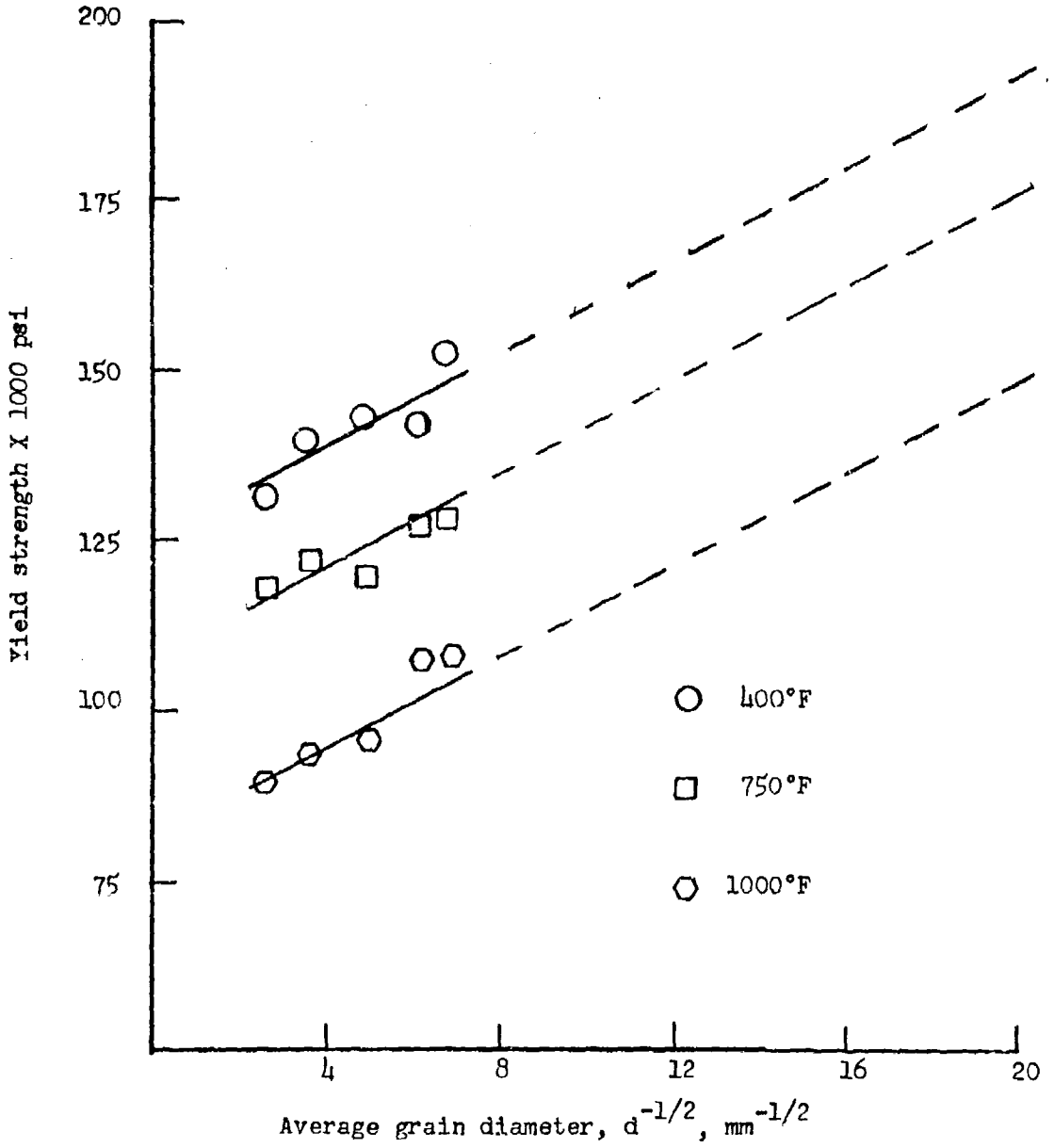

Fig. 15 Temperature and grain size dependence of yield strength of pure tungsten. Instron tests. Four-point loading.

E. Work-hardening Characteristics

It was postulated in Section III that, in addition to the flow stresses of the components, their work-hardening characteristics may also play an important role in the plastic deformation process of the cemented alloys. Therefore, their work-hardening coefficient h was calculated from

$$\epsilon = \left[\frac{\sigma}{h}\right]^2$$

using the plastic region of the stress-strain curve for a few grain sizes. The results for pure tungsten and for the matrix alloy of composition 24W-76(7Ni-3Fe) are summarized in Table II. These values are only approximate due to the nature of the tests, but they give a rough indication of the work-hardening characteristics of the components.

F. Electron Microprobe Analysis

The results of the electron microprobe analysis of the cemented alloys are summarized in Table III. The results are self-consistent in that there is no appreciable difference in the solid solubility of tungsten in the nickel-iron rich matrix regardless of the over-all tungsten content of the alloy. Also, this limit is 24 per cent tungsten, as against 18 per cent reported in the first investigation. The nickel-to-iron ratio remained fairly close to 7:3 in the cemented alloys.

In a separate experiment, a careful scan was made of the variation of tungsten content across a tungsten grain-matrix interface. The readings were taken at one micron intervals, and these intervals were decreased to 1/3 micron near the interface. The results indicated a sudden drop in tungsten content from the grain to the matrix at the interface and no gradual change in composition. The results are plotted in Fig. 16.

When the nickel-iron ratio in the cemented alloy was changed to 6:4, small traces of a new phase, Fe_3W_2, were observed with this instrument.

"Delivered by Armour Research Foundation of Illinois Institute of Technology pursuant to Contract No. DA-11-022-505-ORD-3092. Government's use controlled by the provisions of Articles 26 and 27 of Title II (General Provisions)."

TABLE II

Work-hardening Coefficients of Pure Tungsten and of Matrix Alloy 24W-76(7Ni-3Fe) at Different Temperatures

Temperature °F	Work hardening Coefficient, h, in psi	
	Pure Tungsten	Matrix
Room	brittle	11.8×10^2
400	brittle	10.2×10^2
750	10.1×10^2	10.5×10^2
1000	8.8×10^2	9.2×10^2

TABLE III

Chemistry of Matrix Alloy
as Determined by Electron Microprobe Analyzer

Nominal Composition	Structure	Tungsten in Matrix Alloy
10W-90(7Ni-3Fe)	Single phase	10.1
15W-85(7Ni-3Fe)	Single phase	14.9
18W-82(7Ni-3Fe)	Single phase	17.8
20W-80(7Ni-3Fe)	Single phase	20.2
22W-78(7Ni-3Fe)	Single phase	21.8
24W-76(7Ni-3Fe)	Single phase	24.1
26W-74(7Ni-3Fe)	Single phase	24.2
28W-72(7Ni-3Fe)	Single phase	23.9
80W-20(7Ni-3Fe)	Cemented	24.3
85W-15(7Ni-3Fe)	Cemented	24.5
90W-10(7Ni-3Fe)	Cemented	24.2
91W- 9(7Ni-3Fe)	Cemented	23.9
93W- 7(7Ni-3Fe)	Cemented	24.2
95W- 5(7Ni-3Fe)	Cemented	24.3
96W- 4(7Ni-3Fe)	Cemented	24.1

"Delivered by Armour Research Foundation of Illinois Institute of Technology pursuant to Contract No. DA-11-022-505-ORD-3092. Government's use controlled by the provisions of Articles 26 and 27 of Title II (General Provisions)."

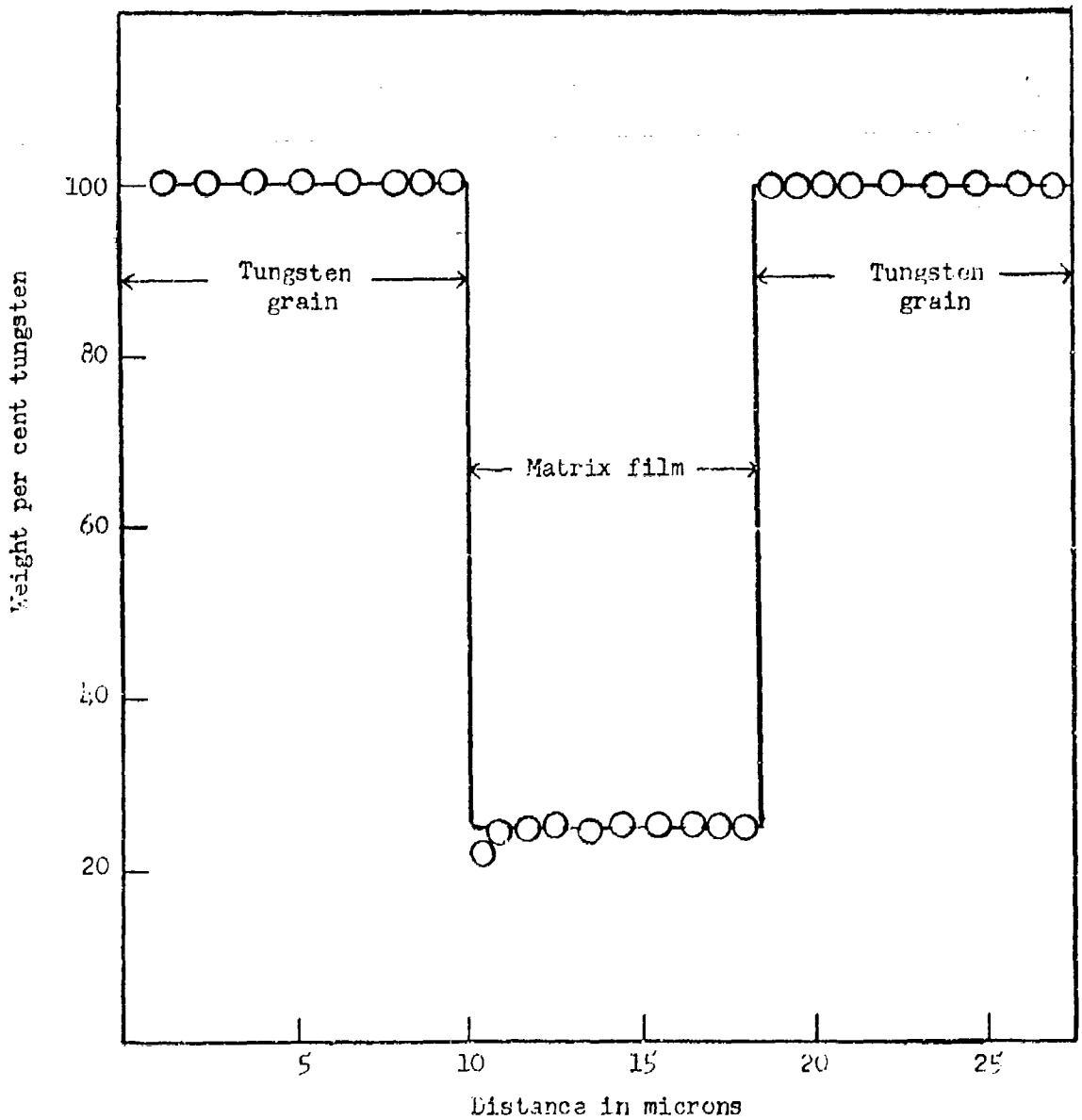

Fig. 16 Electron microprobe scan of tungsten content of grains and matrix in a typical sample of cemented alloy of composition 90W-10(7Ni-3Fe).

This phase could hardly be observed with a metallograph. It appeared as a discontinuous light green phase and had no embrittling effect on the alloys.

G. Residual Stresses from X-Ray Work

By the techniques described in Section IV, the lattice parameters of the matrix alloy were measured for a variety of compositions. The parameter measurements were made on "as-sintered" samples, polished samples, and polished, etched samples. The results are summarized in Table IV. In all cases, the matrix alloy 24W-76(7Ni-3Fe) was used as a standard of lattice parameter in the unstrained condition. Due to the small percentages of the matrix alloy in the cemented structures, the intensities of reflections were low. However, the technique described in Section IV gave reproducible results.

The residual stresses on the matrix were calculated from the simple relationship:

$$\sigma_1 + \sigma_2 = -\left(\frac{E}{\nu}\right)\left(\frac{d_s - d_u}{d_u}\right)$$

where σ_1 and σ_2 are principal residual stresses

E is modulus of elasticity

ν is Poisson's ratio

d_s is lattice parameter of the matrix in cemented alloy

d_u is lattice parameter of single-phase matrix alloy

The residual stresses in the matrix of cemented alloys are plotted in Fig. 17 as a function of volume per cent matrix. The results are reproducible and, therefore, quite reliable.

The residual stresses in tungsten grains of the cemented alloys are plotted in Fig. 18. They are much smaller in magnitude, probably because of the large grain size of tungsten. The relationship between weight and volume per cent tungsten in these cemented alloys is shown in Fig. 18a.

"Delivered by Armour Research Foundation of Illinois Institute of Technology pursuant to Contract No. DA-11-022-505-ORD-3092. Government's use controlled by the provisions of Articles 26 and 27 of Title II (General Provisions)."

TABLE IV

Lattice Parameters of Matrix Alloy and Tungsten Grains as a Function Composition in the Cemented Structure. Samples were Polished and Etched.

Nominal Composition	Structure	a_o (A) Matrix	a_o (A) Tungsten
24W-76(7Ni-3Fe)	Single Phase	3.594	
80W-20(7Ni-3Fe)	Cemented	3.602	3.164
85W-15(7Ni-3Fe)	Cemented	3.601	3.165
90W-10(7Ni-3Fe)	Cemented	3.600	3.167
93W- 7(7Ni-3Fe)	Cemented	3.592	3.167
96W- 4(7Ni-3Fe)	Cemented	3.592	3.166
Pure Tungsten			3.165

"Delivered by Armour Research Foundation of Illinois Institute of Technology pursuant to Contract No. DA-11-022-505-ORD-3092. Government's use controlled by the provisions of Articles 26 and 27 of Title II (General Provisions)."

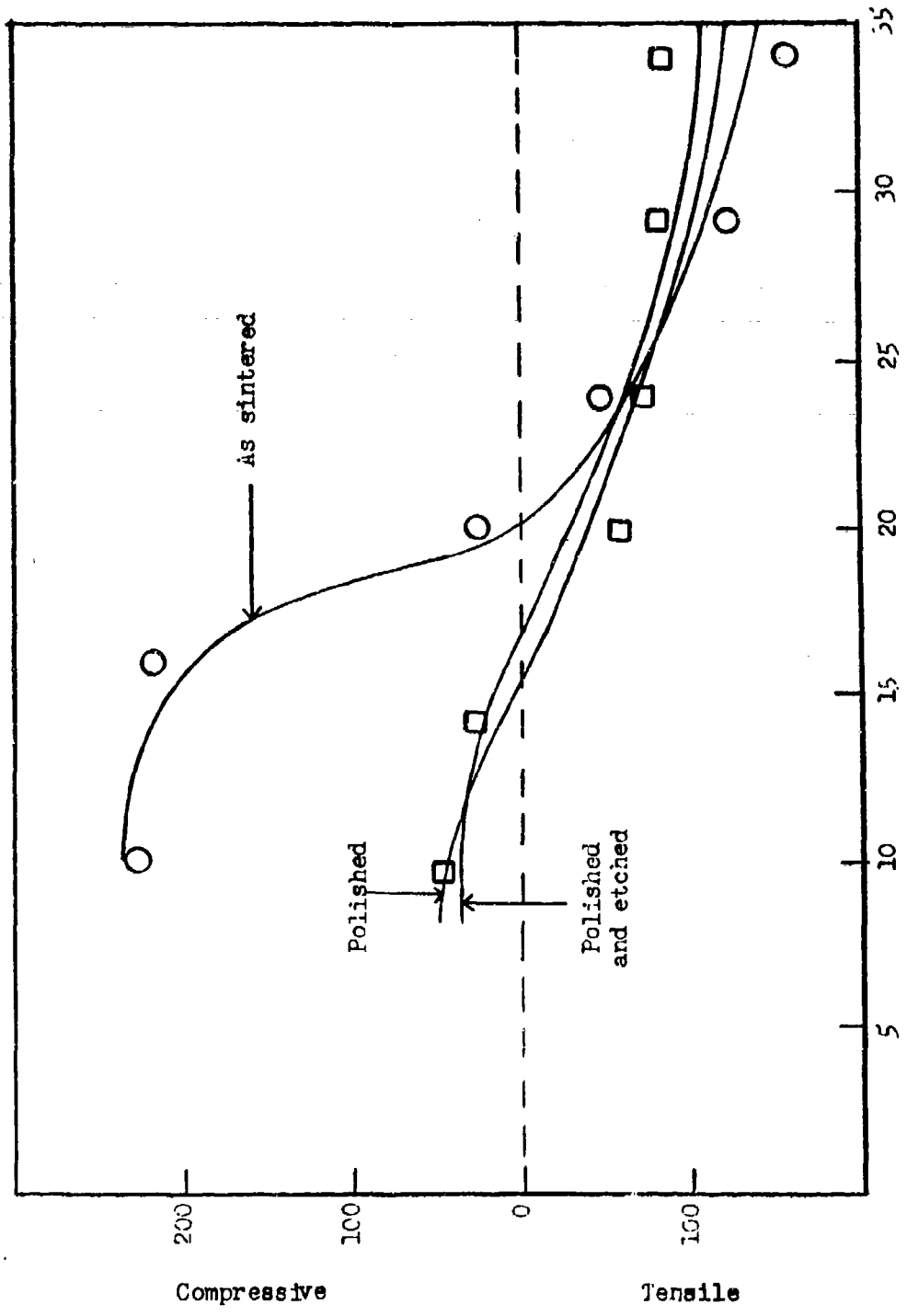

Fig. 17 Residual microstress in matrix phase of cemented W-Ni-Fe alloys with nickel to iron ratio of 7:3. Calculated from X-ray measurements.

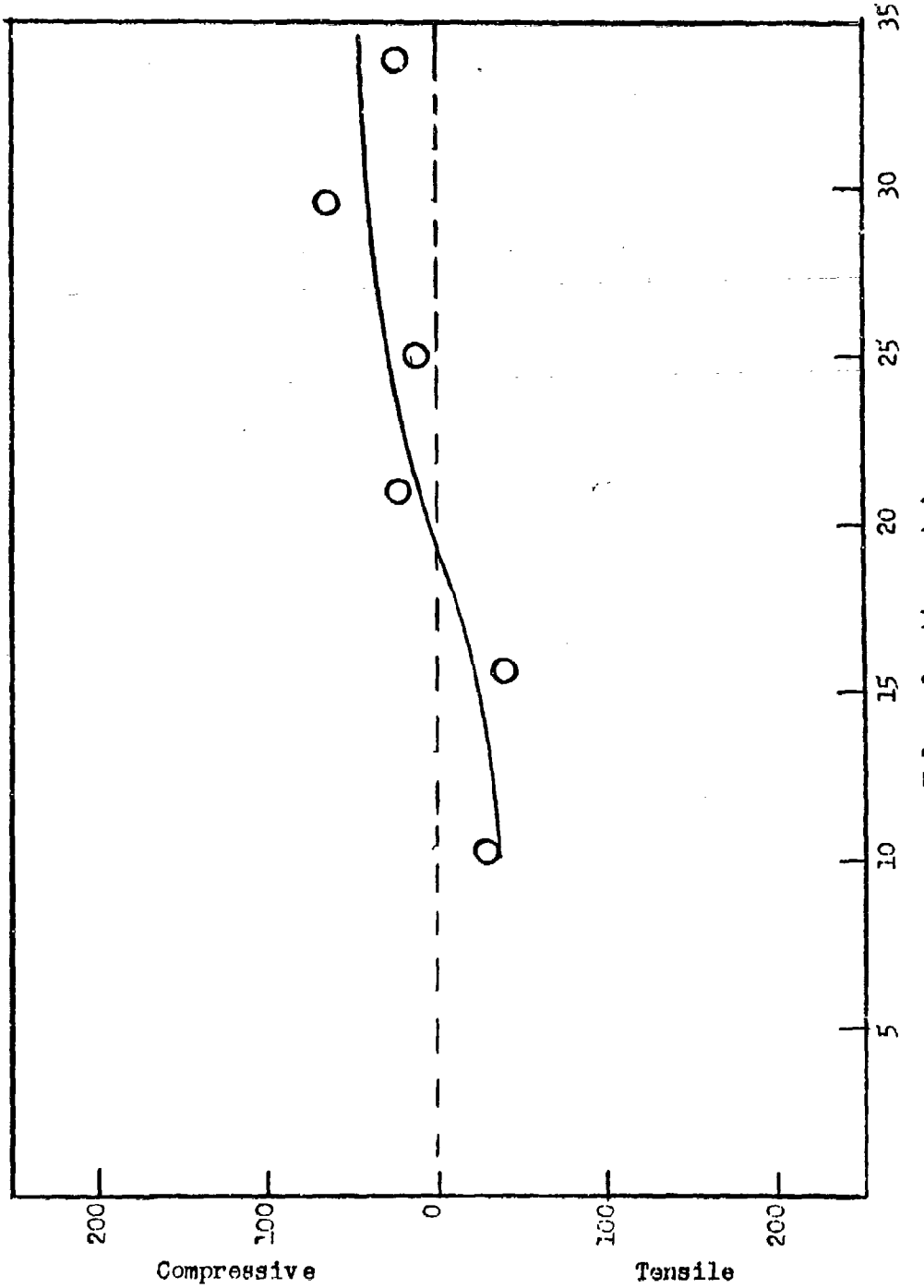

Principal residual stresses on tungsten grains X 1000 psi

Fig. 18 Principal residual microstresses in matrix phase of cemented W-Ni-Fe alloys with nickel to iron ratio of 7:3. Calculated from X-ray measurements.

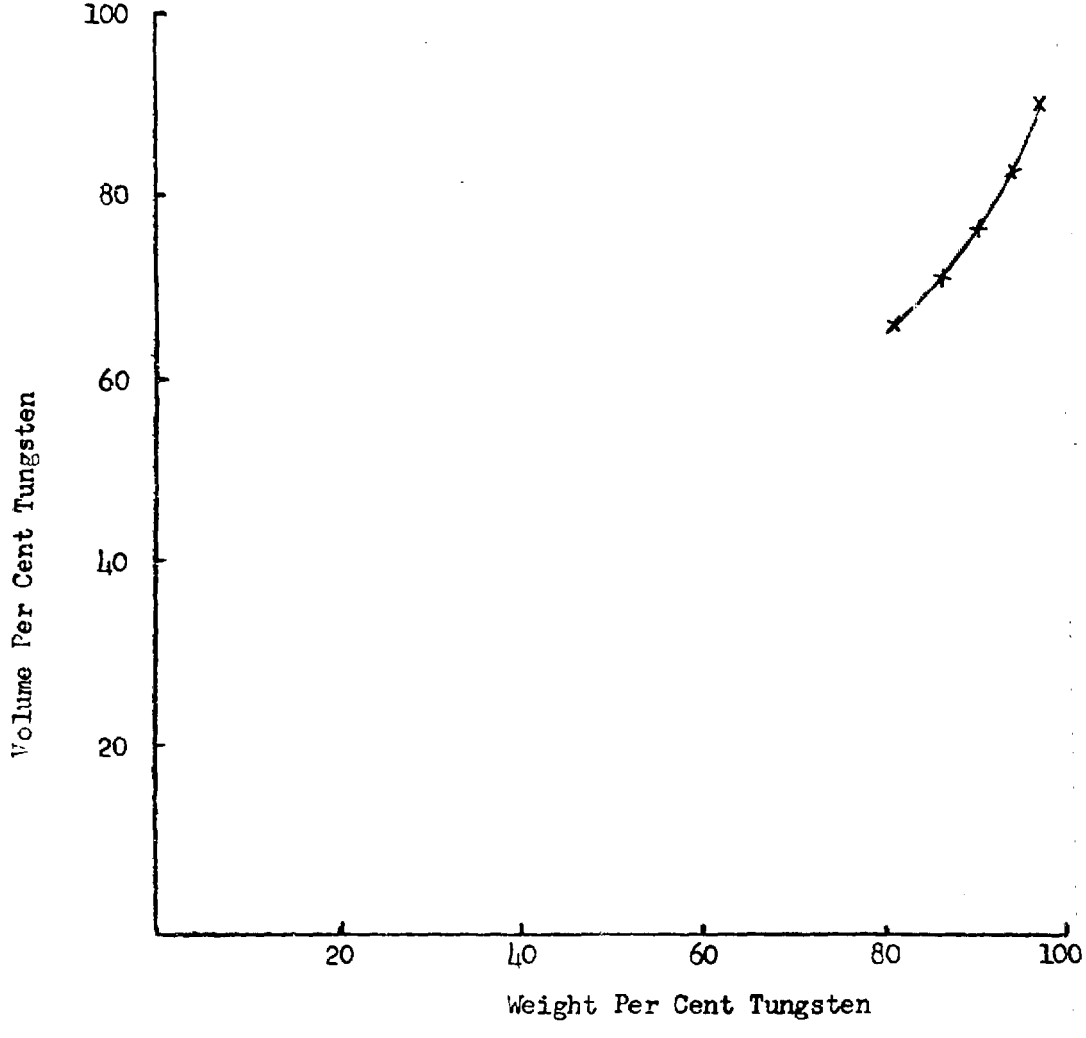

Fig. 18a RELATIONSHIP BETWEEN WEIGHT AND VOLUME PER CENT TUNGSTEN IN CEMENTED TUNGSTEN-NICKEL-IRON ALLOYS INVESTIGATED IN THIS PROGRAM

H. Metallographic and Microhardness Work

Typical microstructures of W-Ni-Fe cemented alloys containing 80 to 96 per cent tungsten and balance nickel and iron in a ratio of 7 to 3 are shown in Fig. 19.

Attempts were made to investigate the modes of deformation of these alloys metallographically. The transverse-rupture bars of these alloys were strained to varying degrees prior to fracture. The test pieces were polished prior to testing. It was found that large "pools" of the matrix in these alloys showed a fair number of slip bands prior to reaching the elastic limit. This may well be a simple grain size effect wherein the deformation takes place on a microscopic localized scale. However, once the stress levels increased beyond the elastic limit, there was extensive deformation of the tungsten grains as well as the matrix and the fracture path was equally through the matrix and the grains.

Samples of binary alloy compositions— which had similar microstructures but exhibited very little ductility -- such as 80W-20Ni and 80W-20Cu were also tested in a similar manner. In the Ni-W system, deformation seemed to be more predominant in the tungsten grains, and the fracture path was also mostly through the grains. In the Cu-W system, however, deformation was only slight through the copper phase (the tungsten deformed not at all), and the fracture path was almost entirely through the copper phase. It was not possible to obtain good photomicrographs because of the displacement of large amounts of material from the plane of the polished surface.

For the series of W-Ni-Fe alloys containing varying percentages of tungsten, the metallographically observable parameters are summarized in Fig. 20. Here the average sintered tungsten grain size and average interparticle separation (matrix film thickness) is plotted as a function of per cent total tungsten.

"Delivered by Armour Research Foundation of Illinois Institute of Technology pursuant to Contract No. DA-11-022-505-ORD-3092. Government's use controlled by the provisions of Articles 26 and 27 of Title II (General Provisions)."

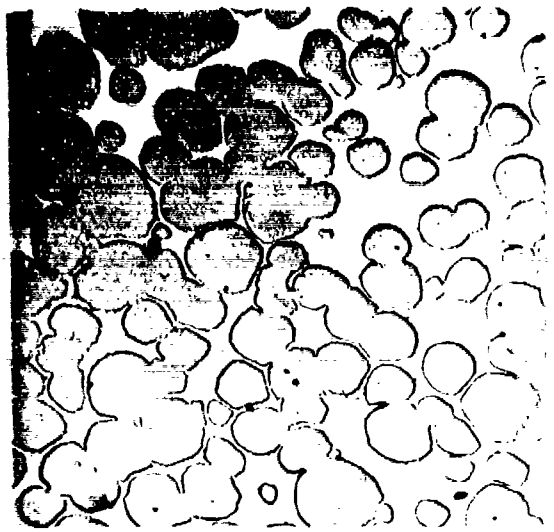

500X

Fig. 19(a) Neg. 19896
85 per cent tungsten

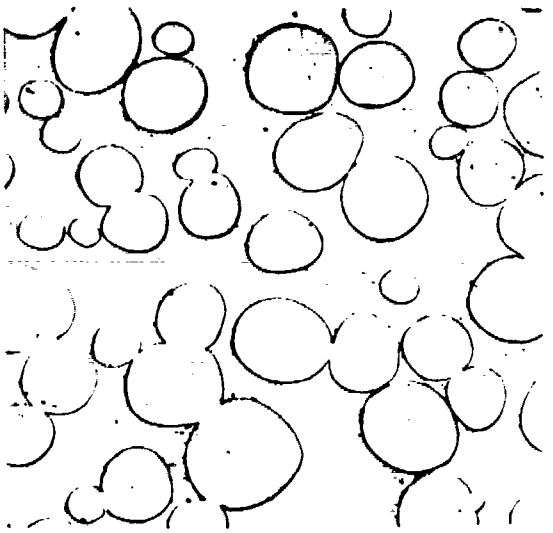

500X

Fig. 19(b) Neg. 19894
80 per cent tungsten

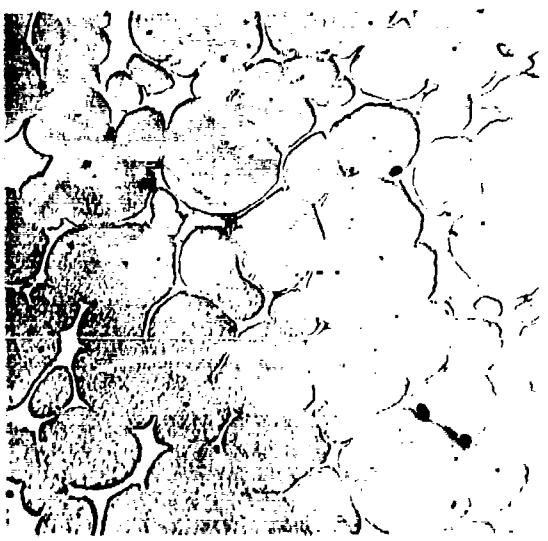

500X

Fig. 19(c) Neg. 19892
90 per cent tungsten

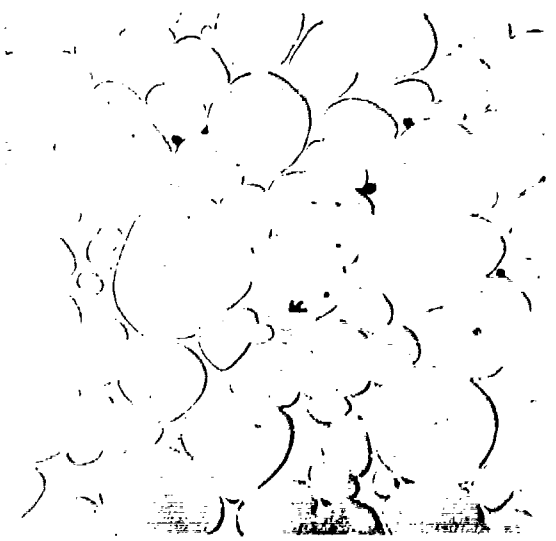

500X

Fig. 19(d) Neg. 19758
93 per cent tungsten

Fig. 19 Microstructures of cemented alloys containing 80 to 93 per cent tungsten and balance nickel and iron in a ratio of 7 to 3.

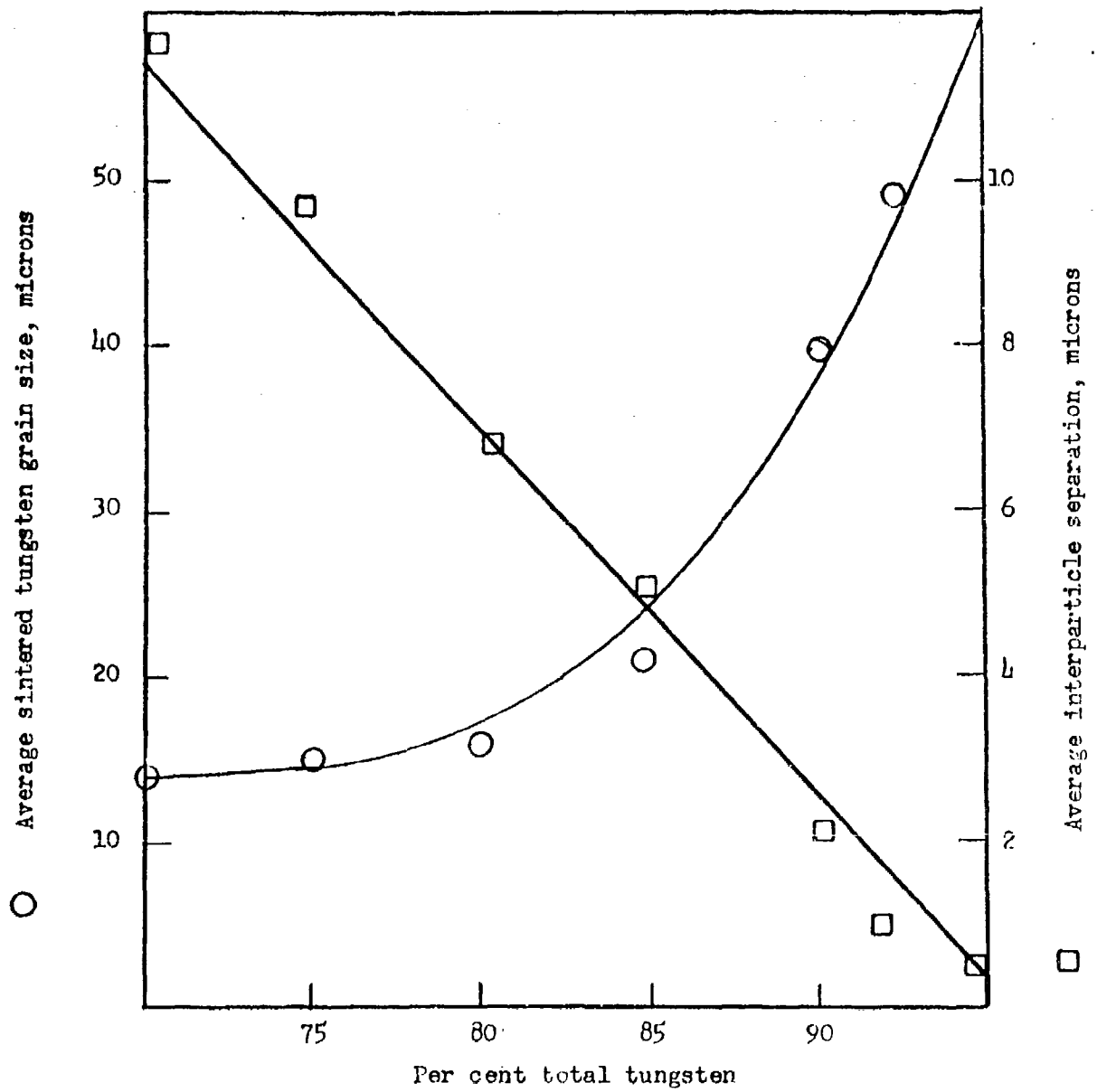

Fig. 20 Sintered tungsten grain size and interparticle separation (matrix film thickness) as a function of total tungsten content in cemented W-Ni-Fe alloys with nickel to iron ratio of 7:3.

The separations between adjoining particles were measured by using a Hurlbut counter in conjunction with a micrometer "Filar" eyepiece. A plot of interparticle separation (matrix film thickness) versus volume per cent tungsten is reproduced in Fig. 20a.

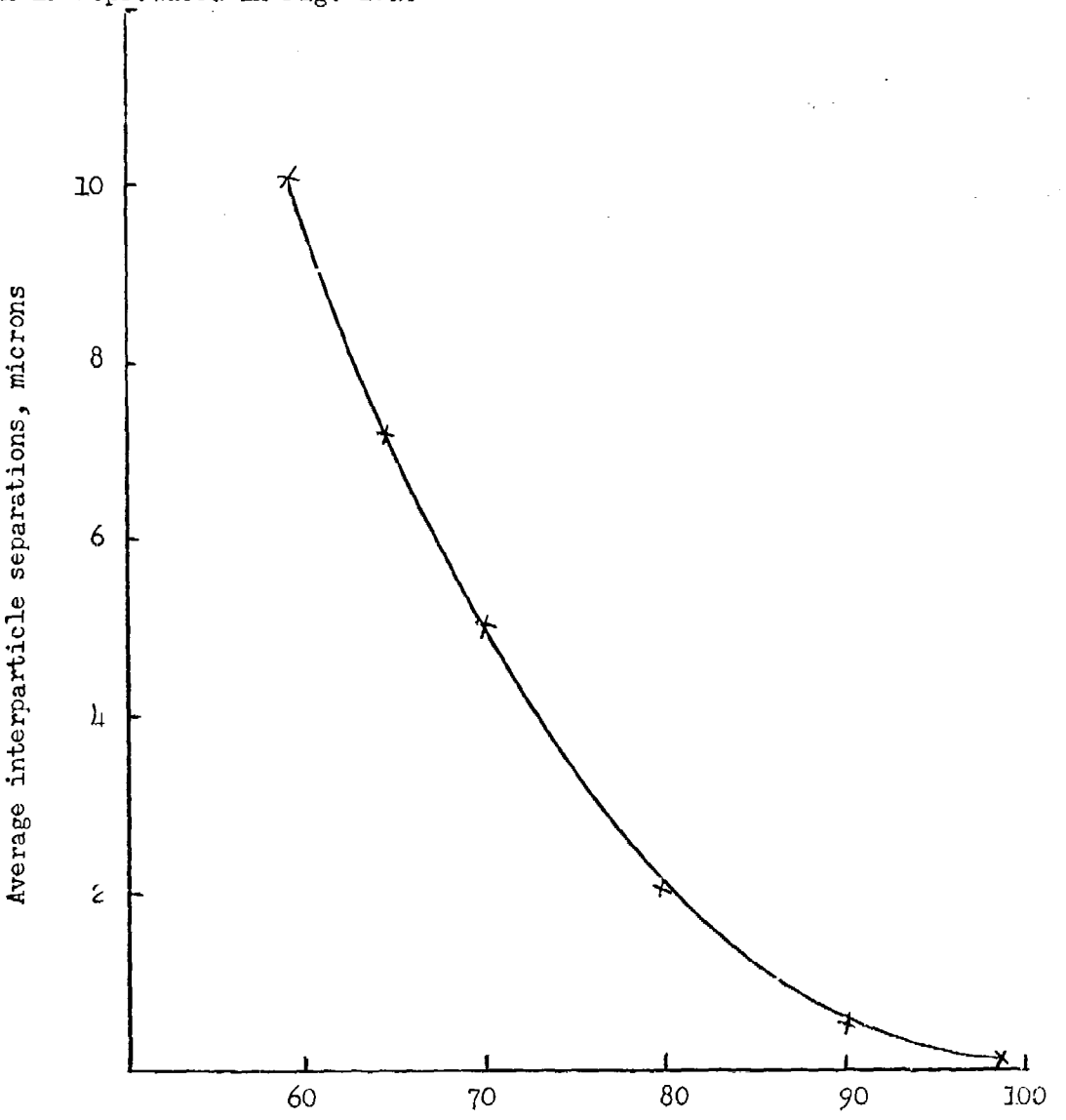

Fig. 20a INTERPARTICLE SEPARATION (MATRIX FILM THICKNESS) AS A FUNCTION OF VOLUME PER CENT TUNGSTEN IN CEMENTED TUNGSTEN-NICKEL-IRON ALLOYS

The density of 24W-76(7Ni:3Fe) matrix alloy is 11.1 gms/cc.

The variation is microcharness of the tungsten grains, as well as the matrix, with varying composition is plotted in Fig. 21.

Several attempts were made to elucidate the state of stress of the tungsten grains in the 90W-10(7Ni-3Fe) alloys. These bars were cold rolled various degrees and polished. The tungsten grains deformed from spherical shape to oval shape after rolling. Careful microhardness measurements of large deformed tungsten grains from the center of the grain to the edge failed to reveal any measurable difference in microhardness. This lack of indication of variation in stress state does not necessarily mean that it is not present. More likely, attempts to measure the stress variation by microhardness failed because the tungsten grains are too small (~ 50 microns) to enable any more than four readings to be made across a grain. The impressions with lowest load (25 gm) range from 9.5 to 10 microns across. Thus the sensivity of such a measurement on the rather small tungsten grains is poor.

In determining the hardness of the matrix in cemented alloy microstructures, we had to restrict ourselves mostly to interstitial areas. For a 25 gm load the minimum matrix film width required for accurate measurements would be about 10-12 microns for alloys studied.

Attempts were also made to study microhardness variations with a diamond scratch hardness indenter. In this method, the pyramid shaped indenter is replaced by a sharp pointed indenter and after a 25 gm load is applied on the selected area of the sample, the micrometer stage is slowly moved to make a long scratch on the surface of the sample. The load is then removed and the scratch width is measured over the different phases exposed on the surface. Initial experiments on polished surfaces exhibited a difference in scratch hardness between matrix and tungsten grains. Further experiments showed that this anomaly was primarily due to the unevenly polished surface. When the samples were electropolished and tested for scratch width, the latter was uniform throughout the two phases. This method is not too satisfactory for measuring hardness variations in two-phase alloys for another reason. The

"Delivered by Armour Research Foundation of Illinois Institute of Technology pursuant to Contract No. DA-11-022-505-ORD-3092. Government's use controlled by the provisions of Articles 26 and 27 of Title II (General Provisions)."

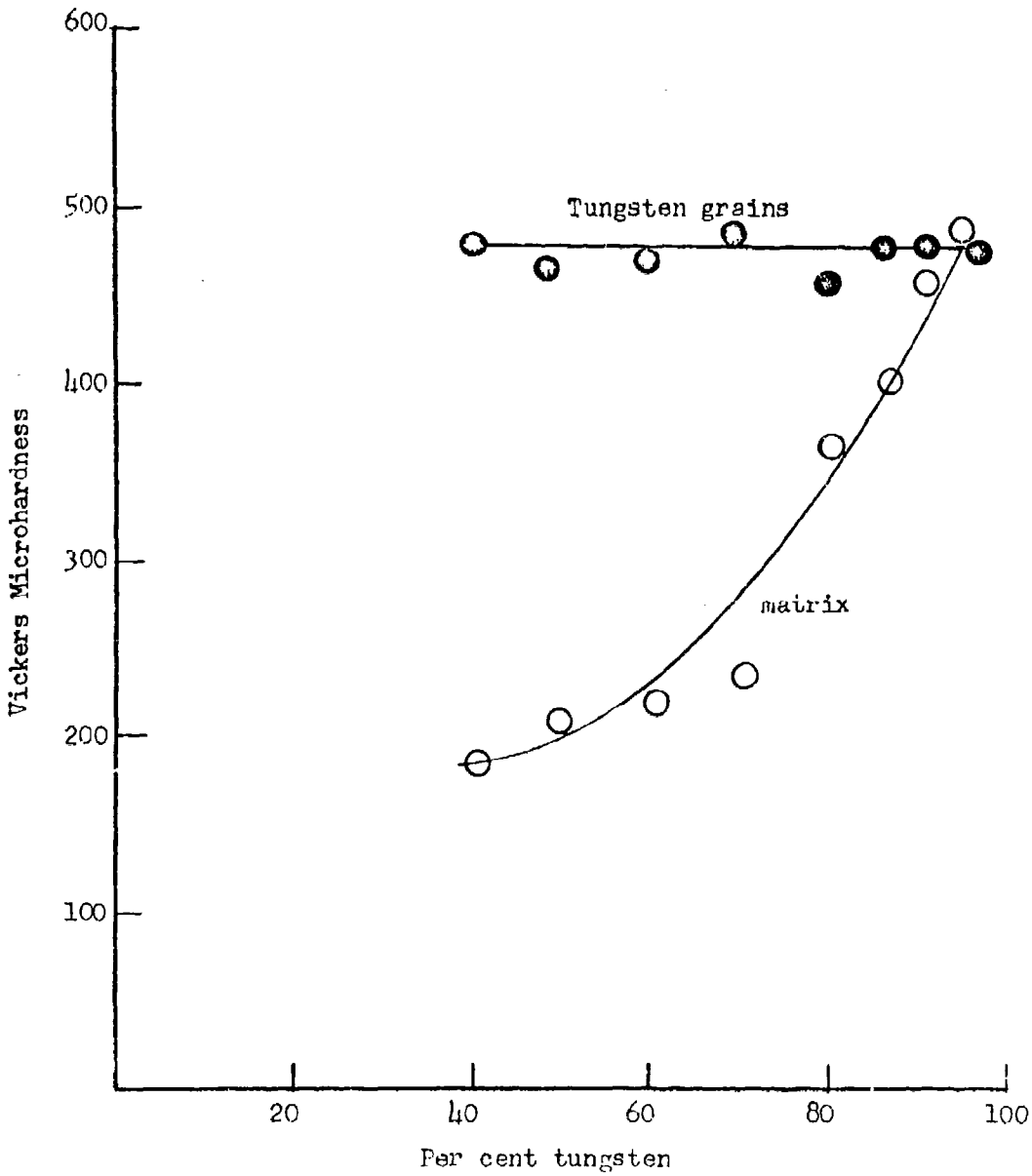

Fig. 21 Variation in microhardness of matrix and tungsten grains as a function of total tungsten content in cemented W-Ni-Fe alloys. Measurements made by using a 25 gm load.

scratch width is too large for the cross section of the matrix. The scratch widths for 25 gm load were about 10 microns in both phases whereas the matrix film thickness was much smaller.

VI. DISCUSSION OF RESULTS AND APPLICATION

The yield strength-grain size relationship in pure tungsten and matrix alloy has provided valuable data which can be correlated in two different ways. Figure 22 consolidates the results of Figs. 13 and 15. When the results for pure tungsten and matrix alloy are extrapolated to the micron size range, it is found that, within a broad scatter band, the flow stresses of the two components match reasonably well. A more acceptable way of plotting these results might be to correlate the "effective" grain size of the matrix and the yield strength. In this case (Fig. 23), the yield strength of the cemented alloys is plotted as a function of matrix film thickness (termed "effective" matrix grain size) and yield strength of the single phase matrix alloy as a function of recrystallized grain size. From many previous investigations, this extrapolation is justified; therefore, such a "size" effect becomes all-important in determining the mechanical properties of two-phase "cemented" alloys. At elevated temperatures, the alloys containing more than 90 per cent tungsten exhibit the mechanical properties of pure tungsten in that their yield strength is essentially constant from 400° to 1000°F and their deflection increases. This behavior is characteristic of pure tungsten in the brittle-ductile transition temperature region. These alloys also exhibit poorer room-temperature ductility as tungsten content increases.

The meager data on work-hardening coefficients (Table II) also indicate that the matrix alloy and tungsten work harden to about the same degree for equal strains, and this would certainly enhance the ductility of these alloys. The plastic region of the stress-strain curves for the matrix alloy and for tungsten over a large range of grain sizes exhibits slopes which are almost identical for equivalent temperatures.

"Delivered by Armour Research Foundation of Illinois Institute of Technology pursuant to Contract No. DA-11-022-505-ORD-3092. Government's use controlled by the provisions of Articles 26 and 27 of Title II (General Provisions)."

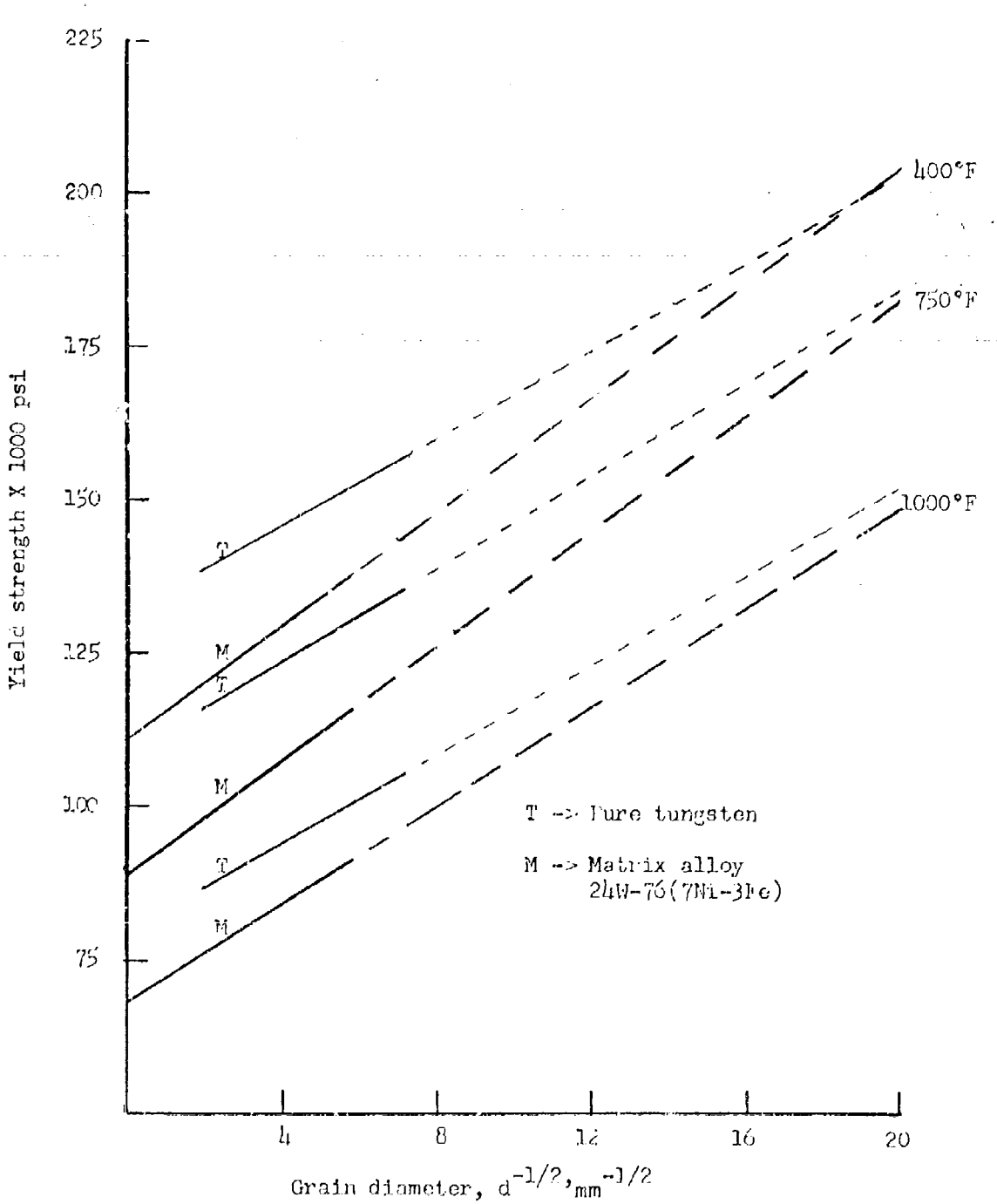

Fig. 22 Temperature and grain size dependence of yield strength of individual components of cemented W-Ni-Fe alloys. Instron tests. Four-point loading. Consolidation of Figs. 13 and 15.

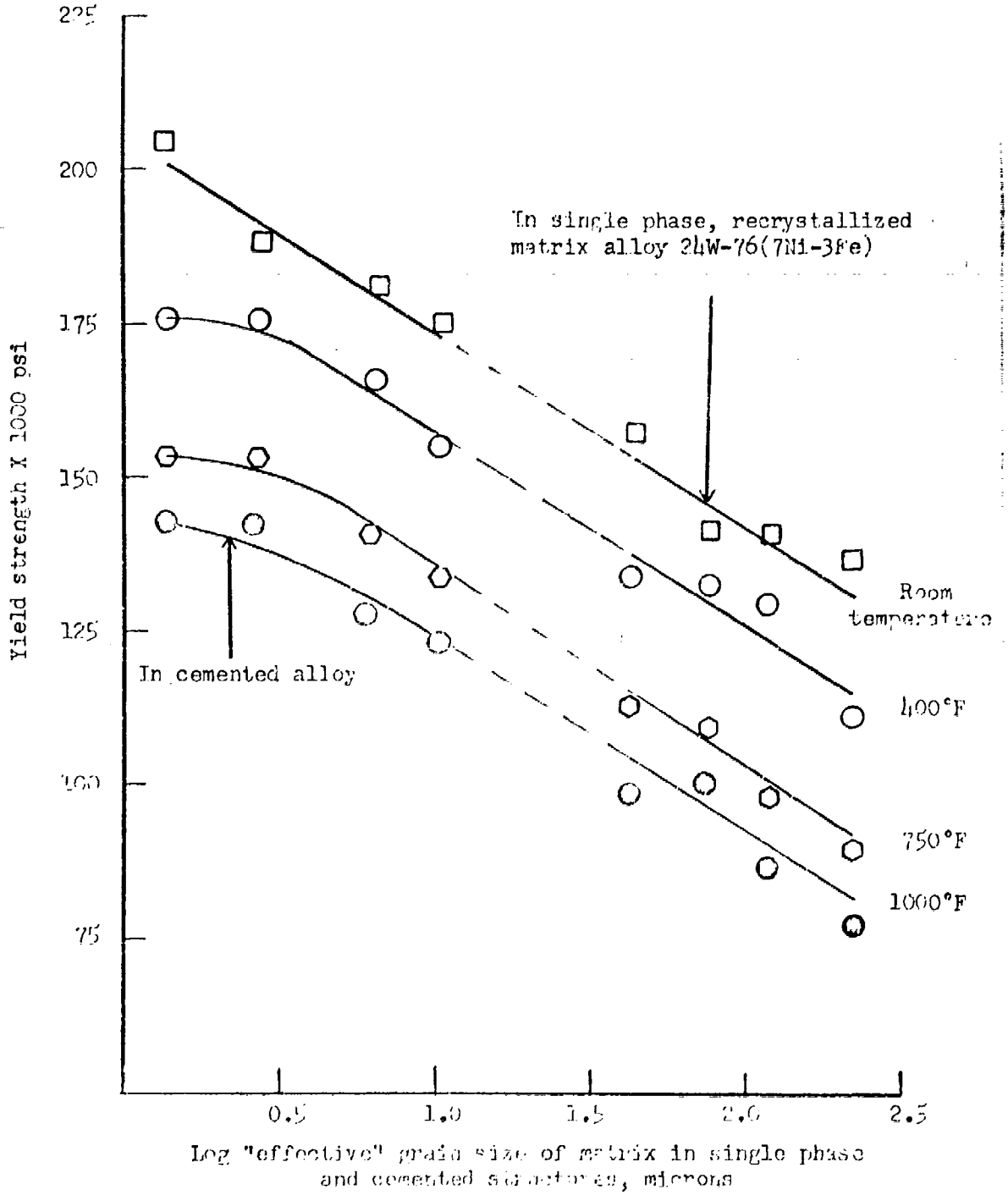

Fig. 23 Yield strength vs. effective grain size of matrix compared with single-phase matrix alloy and matrix alloy in cemented structures. Instron tests. Four-point loading.

Microhardness measurements on matrix and grains afford "screening" techniques for developing new alloys. However, for these alloys, precise measurement of microhardness values of matrix becomes a problem because of the very small thickness of the matrix film.

Some conclusion can be drawn from the metallographic observations in relation to the mechanical behavior of these alloys. In the binary alloys of the W-Ni system, in which the flow stress of the Ni-28W matrix alloy is higher than that of the pure tungsten, the deformation in the two-phase alloy above the elastic limit is predominantly restricted to the tungsten grains. Due perhaps to the higher flow stresses of the matrix film, cracks would be nucleated in the deformed tungsten grains at the grain-matrix interface by dislocation pile-up, and a predominantly transgranular fracture through the tungsten grain results. The same argument is valid for the alloys in the W-Cu system except in reverse because of the low flow stresses of the copper matrix relative to the tungsten grains.

In the W-Ni-Fe cemented alloy system, however, the flow stresses of the matrix and tungsten grains are quite similar. The deformation must start in the weaker of the two phases; but since the flow stresses of the two phases are similar, there would be no major barrier to propagation of slip from one phase to another. This means that there would be no major source of crack nucleation and the two phases would deform simultaneously. As discussed in the previous section, attempts to detect any microhardness gradations in the deformed tungsten grains were unsuccessful.

The electron microprobe analysis helped in establishing the chemistry of the matrix alloy. It also helped in establishing the fact that there is no composition gradient in the matrix nor any measurable solubility of nickel or iron in tungsten.

The residual stress measurements on the matrix of the cemented alloys indicate that there is apparently no direct correlation between residual stress and the mechanical properties of these alloys. That the as-sintered alloys show

---

"Delivered by Armour Research Foundation of Illinois Institute of Technology pursuant to Contract No. DA-11-022-505-ORD-3092. Government's use controlled by the provisions of Articles 26 and 27 of Title II (General Provisions)."

a much higher value of residual stress than the polished samples may be connected with the observation that in all such liquid-phase sintered alloys there is a very slight "flow-out" of the matrix to the surface. The true residual stresses in the matrix, as indicated by the measurements on the polished samples, are rather low in magnitude. The measured stresses on tungsten grains are very low; this is because the grains are rather large and the X-rays can only detect the average changes in lattice parameters.

It must be noted that in the method of measuring the residual stresses, the change in 2θ value is measured over a wide area of the sample covering the matrix in the interstices as well as in the films. As the residual stresses reproduced in Fig. 17 were calculated from the average value of 2θ, it was felt that similar calculations from the limiting values of 2θ obtained for each sample may also establish the stresses more representative of the matrix film. These results are plotted in Fig. 24. Curve A is the same as that plotted in Fig. 17. Curves B and C represent the stresses calculated from the maximum and minimum values of 2θ from the 2θ vs intensity scan. It appears that the stresses calculated from the mean 2θ values are not appreciably different from those calculated from the limiting 2θ values. This, of course, does not necessarily mean that the matrix film stresses are of the same order of magnitude as the interstitial matrix stresses. It only points out the difficulties in measurement and interpretation of the results.

The reasons for the reversal of the sign in stresses at certain volume fractions of the matrix are not clear. Theoretically, if one considers a spherical inclusion in an infinite matrix, it can be shown that the radial and tangential stresses in the matrix are of opposite signs and decrease according to the cube power of the distance from the inclusion.[7,8] However, their analysis will apply only to relatively dilute alloys in which the overlapping of the stress fields of neighboring particles is negligible. The interference of stress fields of an array of inclusions has not been analysed except by inference. Sternberg and Sadowsky[9] showed that when

---

"Delivered by Armour Research Foundation of Illinois Institute of Technology pursuant to Contract No. DA-11-022-505-ORD-3092. Government's use controlled by the provisions of Articles 26 and 27 of Title II (General Provisions)."

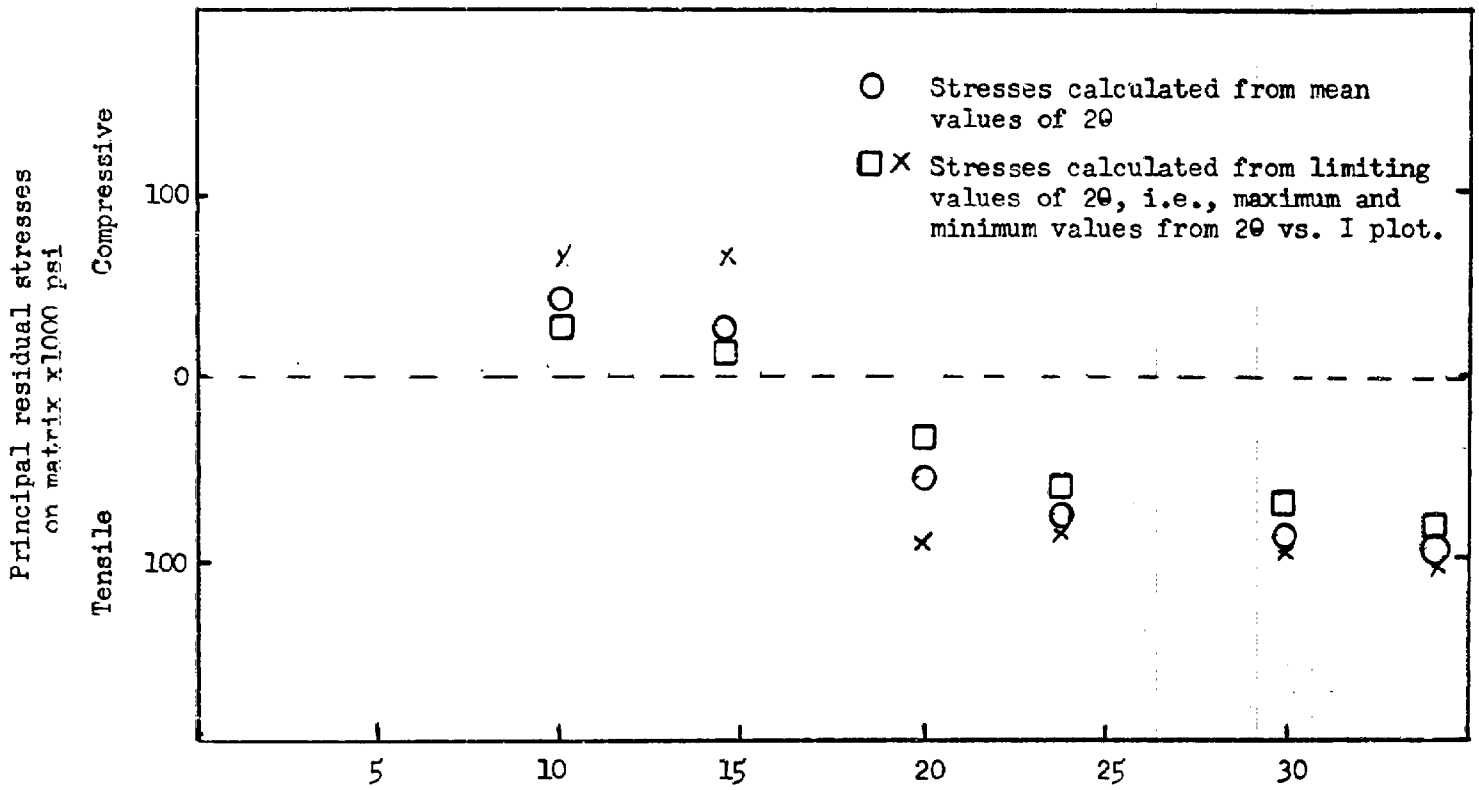

Fig. 24 THE EXTENT OF VARIATION IN MICROSTRESSES IN MATRIX OF TUNGSTEN-NICKEL-IRON ALLOYS AS CALCULATED FROM A RANGE OF 2θ VALUES

the distance between two adjacent cavities (which may be regarded as inclusions) is less than two diameters, the computed stresses deviate drastically from the limiting values. Thus a model based upon spherical inclusions begins to break down as the degree of dispersion of the inclusions decreases. Gurland[7] has concluded by inference that as the degree of dispersion of particles decreases, the stresses in the components become complex and possibly a component of stress of opposite sign is introduced in such a system, thereby causing a sign reversal. This behavior in dispersed alloys makes it almost impossible to evaluate the relationship between residual microstresses and the gross mechanical behavior of two-phase alloys.

The high values of residual microstresses (see Fig. 17) in the as-sintered samples were probably due to the slight "flow out" of the matrix during sintering. This excess concentration of matrix on surface of sintered samples is observed in all samples to a greater or lesser degree. Why this surface in the "as-sintered" condition is so highly stressed is not clear. However, the polished and etched samples show a much lower magnitude of residual thermal stresses--of the order of 50,000 psi in samples containing less than 10 volume per cent matrix--and one would think that these stresses represent truly the internal stress condition in the samples. The mechanical properties of "as-sintered" and polished and etched samples were identical.

The question of "constraint" of the matrix due to triaxial stresses during deformation is still unanswered, and to what degree this phenomenon affects the mechanical behavior of these alloys is not clear. At the moment it seems difficult--if not impossible--to design meaningful experiments which could help in unambiguously elucidating this point.

The concepts developed in this investigation were used for a cursory look at iron-copper alloys with a view to developing high-strength, ductile Fe-Cu alloys. These alloys have a typical cemented alloy structure, but they

---

"Delivered by Armour Research Foundation of Illinois Institute of Technology pursuant to Contract No. DA-11-022-505-ORD-3092. Government's use controlled by the provisions of Articles 26 and 27 of Title II (General Provisions)."

exhibit no ductility, and their strengths in bending are rather low--about 80,000 psi.

The yield strength-grain size relation for pure iron and copper are reproduced schematically in Fig. 25. The curves represent a simple relation:

$$\sigma_y = \sigma_o + k_y d^{-1/2}$$

where σ_y is yield stress

σ_o is stress necessary to initiate motion of unlocked locations,

k_y is magnitude of resistance to motion of dislocations and

d is grain diameter.

Both the values of σ_o and k_y are lower for copper than for iron. Hence, the conclusion must be that there is no chance for ductility in this system. However, there are simple ways of increasing both the σ_o and k_y of copper. One method is by solid solution hardening and the other is age hardening. For solid solution hardening of copper, additions of aluminum, palladium, and manganese were made to Fe-Cu alloys; and for age hardening, small beryllium additions were made. The results of the preliminary investigation of the effects of such additions on the mechanical properties of Fe-Cu alloys are summarized in Table V. It can be seen that most of the additions substantially improved the properties of the Fe-Cu alloys. It was also noted that the manganese additions substantially refined the grain size of the iron particles.

The work on Fe-Cu alloys is by no means conclusive as this phase of the investigation was only cursory. Although comparable properties were

---

"Delivered by Armour Research Foundation of Illinois Institute of Technology pursuant to Contract No. DA-11-022-505-ORD-3092. Government's use controlled by the provisions of Articles 26 and 27 of Title II (General Provisions)."

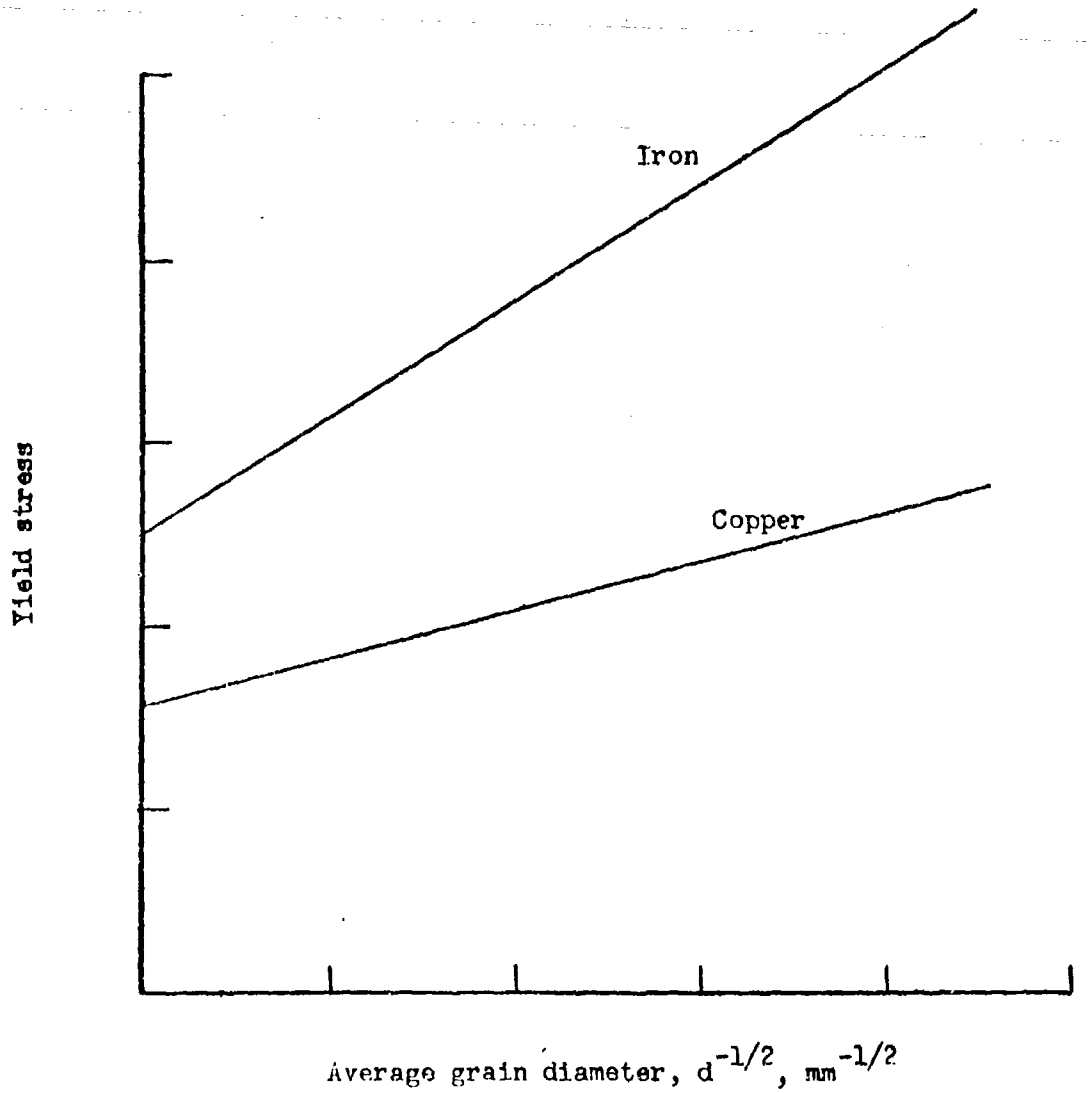

Fig. 25 Schematic representation of yield stress-grain size relationship in iron and copper.

TABLE V

Properties of Some Fe-Cu Base Alloys

Composition	Sintering Treatment	Yield Strength, 1000 psi	Deflection, inches
80Fe-20Cu	1150°C - 1 hr - H_2	60 - 70	None
90Fe-10Cu	1150°C - 1 hr - H_2	85	None
90Fe-10(9Cu-1Al)	1150°C - 1 hr - H_2	130	0.06
90Fe-10(7Cu-3Pd)	1150°C - 1 hr - H_2	175	0.14
80Fe-20(7Cu-3Mn)	950°C - 1 hr - H_2	70 - 82	None
80Fe-20(7Cu-3Mn)	1140°C - 1 hr - H_2	180 - 194	0.1
80Fe-20(7Cu-3Mn)	1200°C - 1 hr - H_2	110	None
80Fe-20(Cu-2Be)	Infiltrated 1300°C Aged 300°C - 1 hr	160 - 175	0.1

"Delivered by Armour Research Foundation of Illinois Institute of Technology pursuant to Contract No. DA-11-022-505-ORD-3092. Government's use controlled by the provisions of Articles 26 and 27 of Title II (General Provisions)."

not realized in the few Fe-Cu alloys investigated, the trend seemed reasonably clear. The matrix-strengthening additions were selected with care so that their diffusion in the particulate phase was very slow at sintering temperatures. If the alloy additions dissolved to any appreciable extent in the iron particles, this dissolution or diffusion was not reflected in the microhardness measurements.

VII. CONCLUSIONS

1. The high strength and ductility of W-Ni-Fe alloys with typical cemented microstructures is primarily due to the similarity in the magnitudes of the flow stresses of the individual components. The particulate phase is almost pure tungsten and the matrix is a nickel base alloy with substantial amount of tungsten dissolved in it during the sintering process. The characteristic flow stresses of the grains and the matrix can be extrapolated from the yield strength-grain size relationship.

2. If the flow stresses of the individual components in cemented alloys are too dissimilar, as in the case of W-Ni or W-Cu binary alloys (with identical cemented structures as in the W-Ni-Fe system), then not only are these alloys brittle, but they also exhibit lower strength values. Thus, in such alloys, the inhomogeneous deformation (or preferential yielding) of the low flow stress component, will build up a stress discontinuities, nucleate cracks, and on further application of stress propagate these cracks to failure at relatively low stress levels. In the W-Ni-Fe system, on the other hand, the response to application of the stress in both components is uniform so that there exists no "barrier" to slip propagation in either of the two phases.

"Delivered by Armour Research Foundation of Illinois Institute of Technology pursuant to Contract No. DA-11-022-505-ORD-3092. Government's use controlled by the provisions of Articles 26 and 27 of Title II (General Provisions)."

3. The work hardening coefficients of the two components in the W-Ni-Fe alloys are fairly similar and this condition is presumed to be important in establishing the degree of ductility. This conclusion is similar to (2) above, but is based upon measurements of work hardening coefficients.

4. The chemistry of the matrix alloy in cemented W-Ni-Fe alloys was established by electron probe measurements. The solubility of tungsten in nickel-iron matrix (7:3 ratio) was found to be about 24 weight per cent at room temperature. Solubility of either nickel or iron in tungsten grains was negligible. Scanning of the phases showed that each phase was of uniform composition.

5. The residual thermal stresses as measured on the components in this system are rather low and, on this basis, are presumed to play a secondary role in determining the mechanical properties of the W-Ni-Fe alloys. As shown in Fig. 24, even if the maximum value of 2θ is used for calculating the d value from which the stresses are calculated, the stresses are calculated, the stresses are rather low and reverse the sign at about 15-20 volume per cent matrix. This does not necessarily mean that matrix stresses are as low as calculated. It demonstrates the difficulty in measuring the matrix stresses in alloys containing such low percentages of the matrix.

6. Metallographic study of fracture behavior supports the developed theory that the two components possess flow stresses of the equivalent flow stresses, as discussed in conclusions (1) and (2) above.

"Delivered by Armour Research Foundation of Illinois Institute of Technology pursuant to Contract No. DA-11-022-505-ORD-3092. Government's use controlled by the provisions of Articles 26 and 27 of Title II (General Provisions)."

7. The concepts developed here were successfully applied to a cursory investigation of the alloys in the Fe-Cu system--- resulting in high-strength alloys with some ductility.

VIII. LOGBOOKS AND CONTRIBUTING PERSONNEL

The data are all recorded in Logbooks Nos. C-9399, C-1089, and C-1180.

N. M. Parikh, J. R. Walenga (Technician), and E. Heckenbach (Technician) contributed to this program.

Respectfully submitted,

ARMOUR RESEARCH FOUNDATION OF
ILLINOIS INSTITUTE OF TECHNOLOGY

N. M. Parikh.

N. M. Parikh, Senior Metallurgist

W. Rostoker

W. Rostoker, ~~Assistant~~ Director
Metals Research

NMP:cs

"Delivered by Armour Research Foundation of Illinois Institute of Technology pursuant to Contract No. DA-11-022-505-ORD-3092. Government's use controlled by the provisions of Articles 26 and 27 of Title II (General Provisions)."

REFERENCES

1. Green, E. C., D. J. Jones, and W. R. Pitkin, Symposium on Powder Metallurgy London, Iron Steel Inst., pp. 1-4, (Dec. 1954)

2. Taylor, G. I., "Plastic Strain in Metals" J. Inst. Metals, 62, 307 (1938).

3. Soldau, P., Z. Anorg. Allgem. Chem., 194, 1 (1930).

4. Honeycomb, R. W. K., and W. Boas, Australian J. Sci. Res., 1, 70 (1948).

5. Clarebough, L. M., Australian J. Sci. Res., 3, 72 (1950).

6. Gensamer, M., "Strength and Ductility" Trans. ASM, 36, 30 (1946).

7. Gurland, J., Trans. ASM, 50, 1063 (1958).

8. Laszlo, F., Jour. Iron and Steel Inst., 147, 173, (1946).

9. Sternberg, F., and Sadowsky, Jour. Appl. Mech., 21, 57, (1954).

"Delivered by Armour Research Foundation of Illinois Institute of Technology pursuant to Contract No. DA-11-022-505-ORD-3092. Government's use controlled by provisions of Articles 26 and 27 of Title II (General Provisions)."

A.D. _____ Accession No. _____

Watertown Arsenal Laboratories, Watertown 72, Massachusetts. DEVELOPMENT AND APPLICATION OF A THEORY OF PLASTIC DEFORMATION OF CEMENTED ALLOYS, by N. M. Parikh. Report No. WAL 372/32. March 1961. pp. 60 - illus. 25 - tables 5, DA Project 11-022-505-ORD-3092, ORD Project No. TB4-002.

Unclassified report

In the cemented W-Ni-Fe alloys, the sources of strength and ductility were found to be due to the close matching of the yield stresses of the matrix and tungsten particles. This was proved by measuring yield strength as a function of grain size of the matrix and tungsten individually. The chemistry of the matrix was established by electron probe analysis. The residual stresses in these cemented alloys were measured by the X-ray method. Applications of these principles resulted in a few new Fe-Cu base alloys of high strength and ductility.

UNCLASSIFIED

A.D. _____ Accession No. _____

Watertown Arsenal Laboratories, Watertown 72, Massachusetts. DEVELOPMENT AND APPLICATION OF A THEORY OF PLASTIC DEFORMATION OF CEMENTED ALLOYS, by N. M. Parikh. Report No. WAL 372/32. March 1961. pp. 60 - illus. 25 - tables 5, DA Project 11-022-505-ORD-3092, ORD Project No. TB4-002.

Unclassified report

In the cemented W-Ni-Fe alloys, the sources of strength and ductility were found to be due to the close matching of the yield stresses of the matrix and tungsten particles. This was proved by measuring yield strength as a function of grain size of the matrix and tungsten individually. The chemistry of the matrix was established by electron probe analysis. The residual stresses in these cemented alloys were measured by the X-ray method. Applications of these principles resulted in a few new Fe-Cu base alloys of high strength and ductility.

UNCLASSIFIED

UNCLASSIFIED

A.D. _____ Accession No. _____

Watertown Arsenal Laboratories, Watertown 72, Massachusetts. DEVELOPMENT AND APPLICATION OF A THEORY OF PLASTIC DEFORMATION OF CEMENTED ALLOYS, by N. M. Parikh. Report No. WAL 372/32. March 1961. pp. 60 - illus. 25 - tables 5, DA Project 11-022-505-ORD-3092, ORD Project No. TB4-002.

Unclassified report

In the cemented W-Ni-Fe alloys, the sources of strength and ductility were found to be due to the close matching of the yield stresses of the matrix and tungsten particles. This was proved by measuring yield strength as a function of grain size of the

UNCLASSIFIED

UNCLASSIFIED

matrix and tungsten individually. The chemistry of the matrix was established by electron probe analysis. The residual stresses in these cemented alloys were measured by the X-ray method. Applications of these principles resulted in a few new Fe-Cu base alloys of high strength and ductility.

UNCLASSIFIED